






Evolution of Seismic Reliability of Code-Conforming Italian Buildings

Iunio Iervolino ^a, Roberto Baraschino ^a, and Andrea Spillatura ^b

^aDipartimento di Strutture per l'Ingegneria e l'Architettura, Università degli Studi di Napoli Federico II, Naples, Italy;

^bDipartimento di Costruzioni e Infrastrutture, Fondazione Eucentre, Pavia, Italy

ABSTRACT

It is well known that the seismic structural reliability is not explicitly controlled in design carried out according to seismic contemporary building codes; that is, those enforcing a simplified version of performance-based design. This is even more true for structures designed with obsolete seismic codes or without any seismic provisions at all, which constitute most of the building stock in countries such as Italy. Between 2019 and 2021, a large research project, RINTC – *Rischio Implicito delle Norme Tecniche per le Costruzioni* (i.e. *implicit risk of existing buildings designed according to the Italian codes*), has addressed, in a coherent manner, the inherent seismic structural reliability of existing Italian structures built according to evolving codes, which have now been superseded by multi-limit-state-based provisions. To this aim, five structural typologies of residential and industrial buildings have been considered, that is, reinforced concrete, pre-cast reinforced concrete, base-isolated reinforced concrete, masonry, and steel structures. The building design accounts for the evolution of codes within the last century or more. Structures are supposedly located at five sites in the country, representative of different seismic hazard, both currently and at the time of design. Nonlinear state-of-the-art three-dimensional numerical models for the considered structures have been analyzed via multi-stripe nonlinear dynamic analysis, the results of which, in turn, have been used to evaluate the annual failure rate as a measure of seismic reliability with respect to two performance levels defined within the project and named *global collapse* and *usability-preventing damage*. These rates, finally, allowed to appreciate the variation of seismic safety with the evolution of codes and to compare with that implied by current design. The results of the study allowed to conclude that the evolution of seismic codes clearly tends to enhance the seismic reliability with the largest average improvement attributable to the enforcement of the current code.

ARTICLE HISTORY

Received 12 November 2021

Accepted 4 May 2022

KEYWORDS

Fragility; design; reinforced concrete; steel; masonry; precast; base isolation; structural safety; seismic hazard

1. Introduction

Building codes provide a series of principles and rules, so that the resulting construction ought to implicitly satisfy some reliability requirements. However, the link between structural reliability goals and design is somewhat loose and the safety achieved is unknown. This is true even for current (i.e. state-of-the-art) codes that enforce multi-limit-state-based design (sometimes also referred to as a simplified version of *performance-based seismic design*), such as the Italian building code, NTC18 (CS.LL.PP 2018). According to the Italian code, which is somewhat similar to the Eurocode (CEN 2004), the design actions (i.e. the ground motion intensity) are determined based on the limit state considered and the corresponding exceedance return period

from probabilistic seismic hazard analysis (PSHA; Cornell 1968) for the construction site. To address this issue, between 2015 and 2017, a large research project, that is RINTC – *Rischio Implicito delle Norme Tecniche per le Costruzioni*, has evaluated the current-code-implied seismic reliability of code-conforming structures in Italy (Iervolino and Dolce 2018). In this first round of the RINTC project, which is by now concluded, buildings belonging to five structural typologies were designed to code, at three locations in the country, spanning a wide range of seismic hazard levels. Nonlinear numerical models of the designed structures were analyzed via nonlinear dynamic analysis and their reliability was evaluated by integrating probabilistic representations of site hazard and seismic structural fragility, thus determining their annual failure rates. The results (Iervolino, Spillatura, and Bazzurro 2018) mainly show that, even if the design seismic actions have the same return period of exceedance at all sites, the implicit seismic reliability of code-conforming structures tends to decrease as the design site's hazard increases. This is due to a combination of the code-prescribed minima (including gravity-load design at the lowest hazard sites; see Baltzopoulos, Grella, and Iervolino 2021) and the effect of ground motions with return period larger than those considered in design (Cito and Iervolino 2020).

Although the implicit reliability of new structures is certainly interesting, it must be recognized that in countries, such as Italy, most of the building stock has been designed with obsolete seismic codes, that is *low-code* buildings, or without any seismic provisions at all, that is *pre-code* buildings (e.g. Petruzzelli and Iervolino 2021). For these constructions, the link between design and reliability is even weaker as the design actions are not directly based on PSHA and the design goals are not performance-based. In fact, the design-implied seismic structural reliability of existing structures, in Italy, has been addressed in a second round of the RINTC project (2019–2021), the results of which are the focus of this paper. In the 2019–2021 RINTC project the same five structural residential and industrial typologies considered for new design were retained, that is: (i) reinforced concrete or RC, which includes some cases where soil–structure interaction is considered (Iovino, Noto, and Di Laora et al. 2022), but that were excluded from the reliability analysis herein, (ii) pre-cast reinforced concrete or PRC, (iii) base-isolated reinforced concrete or BI, (iv) unreinforced masonry or URM, and (v) steel or S. For each typology, design was carried out considering all the major changes in provisions and practice in the last century or more, and it includes cases in which only gravity loads or other non-seismic actions are accounted for. Structures are supposedly located at five Italian sites, representative of different seismic hazard, both currently and at the time of design. As a result, more than one-hundred-forty buildings were designed and for each of them three-dimensional state-of-the-art nonlinear numerical models (benchmarked against real case-studies; Angiolilli, Eteme Minkada, and Di Domenico et al. 2022) were developed and analyzed via multi-stripe nonlinear dynamic analysis, featuring hazard-consistent record selection (Spillatura et al. 2021). This leads to a probabilistic representation of structural seismic vulnerability; that is, the seismic *fragility*. The latter is evaluated with respect to two performance levels defined within the project and named *global collapse* and *usability-preventing damage*. The obtained (parametric) fragility curves, which are made available for further studies, intentionally do not include uncertainty in structural modelling (Jalayer, Elefante, Iervolino et al. 2011 Jalayer, Iervolino, and Manfredi 2010), the possible degradation in time (Iervolino, Giorgio, and Chioccarelli 2013), or other factors, such as construction quality assurance procedures, so as to isolate the effect of design. The fragility curves are integrated with the (current) hazard curves from PSHA for the construction sites, to assess the seismic reliability measured in terms of annual failure rates. These rates, finally, allowed to appreciate the variation of seismic safety with the evolution of codes and to compare with that implied by current design, as addressed by the 2015–2017 RINTC project.

To illustrate the study, the remainder of the paper is structured such that a recap of the major steps in the evolution of design codes and design seismic actions in Italy is given first. Second, the structural typologies and the considered buildings are briefly described, redirecting the interested reader to specific papers for more details. Third, the methodology for the nonlinear dynamic analysis and the seismic fragility/reliability assessment of the building models are discussed, along with the sites' probabilistic seismic hazard analysis. Some final remarks close the paper, while an appendix contains the parameters of the lognormal fragility curves and rates of failure for all the buildings considered.

2. Evolution of Design Codes

In Italy, not considering masonry structures, a large part of the buildings was designed between the '60s and '70s, a period when only a fraction of the Italian territory, ranging between 15% and 35%, was considered to be seismically prone for structural design purposes, as will be discussed in the following. In fact, seismic regulatory codes in Italy have undergone a significant number of changes in the last century that, until very recently, were typically enforced in the aftermath of catastrophic seismic events. This section will provide a summary overview of this topic, while the interested reader should refer to Petruzzelli and Iervolino (2021) and references therein, for a more comprehensive and informative review.

The Royal Decree (*Regio Decreto*) no. 193 of 04/18/1909 (*Regio Decreto 1909*), came into effect after the *Messina Strait earthquake* of 1908 (moment magnitude, M_w , 7.1), and is usually referred to as the first documented national Italian seismic building code. It contained instructions to be applied in the most heavily stricken areas, which were also defined as *seismic zones*. In fact, in order to control the seismic vulnerability of new constructions, some limitations about building height (i.e. height lower than 10 m, storey number lower or equal than two, maximum storey height of 5 m) and other provisions for different structural typologies, were given. The first explicit provision regarding the value of the horizontal seismic base shear (i.e. the so-called *seismic coefficient*) was introduced in 1915 with the royal decree no. 573 of 04/29/1915 (*Regio Decreto Legge 1915*), after the *Avezzano earthquake* in the Abruzzo region (M_w 7). According to the royal decree no. 431 of 03/13/1927, a lower level of seismic base shear and less restrictive structural provisions were introduced for sites considered to be of moderate seismicity. In those zones, belonging to the so-called *second category* or *category II*, the seismic action was different from the one specified for buildings located in highly hazardous sites (*first category* or *category I*). The royal decree no. 640 of 03/25/1935 (*Regio Decreto Legge 1935*) reduced the horizontal seismic forces in category I and II, respectively. The assumption of a constant distribution of forces along the building height, independently from the seismic category, was established in 1935 and remained unchanged up to 1975. Moreover, in 1937 (*Regio Decreto Legge 1937*) the seismic coefficient for category II was further reduced. The 1962 code (*Legge 25 novembre 1962*) regionally changed again horizontal seismic forces.

A major step in the evolution of seismic codes in Italy was the law no. 64 of 02/02/1974 (M.LL. PP. 1974), which established the administrative framework of seismic regulations in Italy, entrusting the periodical updating of technical provisions to the government. The ministry decree no. 40 of 03/03/1975 (*Decreto Ministeriale 1975*) was the first code issued in accordance with the mentioned law and introduced significant changes in Italian seismic provisions. More specifically, it introduced the *response spectrum* and, additionally, dynamic or static analyses were given as design options. After the *Irpinia earthquake* in 1980 (M_w 6.9), a third seismic category was introduced (*Decreto Ministeriale 1981*). A further evolution of Italian regulatory provisions saw the definition of an *important factor* in 1984 (*Decreto Ministeriale 1984*), in order to amplify the design base shear.

Up to 1996 the only design approach was based on *admissible stress*, that is, conventional elastic analysis at the material level. In 1996 (*Decreto Ministeriale 1996*) limit state design was introduced. However, the admissible stress approach, by virtue of being much more familiar to practitioners, was still allowed, so that the limit state design was largely dismissed in practice. Moreover, the instruction document related to the 1996 code (M.LL.PP. 1997), contained the first indications in the direction of capacity design aiming to improve local and global ductility.

The 2003 seismic code (OPCM 3274 2003), and its subsequent modifications (OPCM 3431 2005), represented the most significant change in Italian seismic provisions in over 30 years. The Eurocode 8 approach was acknowledged, and a fourth seismic zone was introduced. An elastic response spectrum with a fixed shape (depending on local geology), anchored to a conventional *peak ground acceleration* (PGA), was enforced. Reference PGA values for the four zones were 0.35 g, 0.25 g, 0.15 g, and 0.05 g for zones from 1 to 4, respectively. Each site fell in one of the four zones depending on the PGA, on rock,

with an exceedance return period of 475 years, evaluated by means of PSHA. The elastic response spectrum had to be modified as a function of the *behavior factor*, q , to get the (inelastic) design spectrum required by some analysis methods. This code also enforced *capacity-design* (Fardis 2018) principles.

The next-to-latest regulation update, NTC08 (CS.LL.PP. 2008), finally enforced a simplified version of performance based design (see Vamvatsikos 2017, for a discussion), after L'Aquila earthquake in 2009. A major novelty of the NTC08 was that seismic hazard was completely site-specific and based on PSHA (see the following section). In 2018, a revision of the NTC08 was released, which was already indicated herein as NTC18, without substantial changes in the definition of elastic seismic actions on structures.

2.1. Evolution of Seismic Classification (Design Hazard) and Chosen Sites

Since 1909, the complex task of mitigating the seismic risk in Italy was entrusted to seismic building codes in conjunction with the seismic classification, defining which areas of the Italian territory were to be considered seismically hazardous in a relative sense. In several cases, up until the '70s a region was considered to be seismically prone only after the occurrence of a seismic event. This aspect clearly emerges from Fig. 1, where a few steps in the evolution of seismic classification are shown.¹

A law of 1962 (Legge 25 novembre 1962) stated that seismic design should be applied to municipalities subject to *intense seismic activity*, but until the early '80s this prescription remained substantially unattended. In 1974 (M.LL.PP. 1974) the need to classify the territory on the basis of *proven technical reasons* was reaffirmed, and in 1979 *macroseismic intensity* maps were used as a basis for the identification of seismic zones. This led to issue several decrees aimed at the territorial seismic classification between 1979 and 1984 (Di Pasquale et al. 1999), so that, at the end of 1984, 37% of municipalities and 45% of the Italian territory was considered to deserve seismic design. The 2002 earthquake in San Giuliano di Puglia (Mw 5.8), which caused the death of twenty-seven students and their teacher in a school, dramatically brought to attention the lack of updates of the seismic classification of the Italian territory (Pinto et al. 2003), which had remained the same since 1984. Therefore, a minimal level of seismic design was ensured for the entire country. In the following years, thanks to the work of the *Istituto Nazionale di Geofisica e Vulcanologia* (INGV) (Stucchi et al. 2011), a PSHA was performed for several spectral ordinates at each point of a fine grid, covering the whole Italian territory (except the Sardinia region). Moreover, design elastic response spectra were defined starting from *uniform hazard spectra*, computed as a function of the geographical coordinates of the site, which is the current approach.

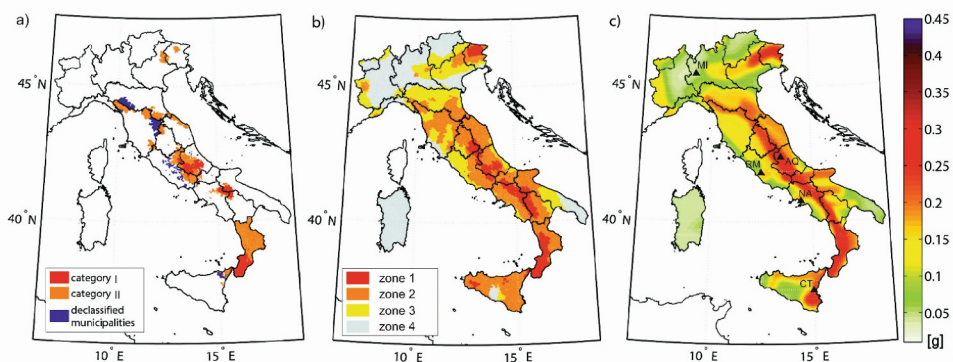


Figure 1. Italian seismic actions maps in: 1937 (left), 1984 (center), today (right). Adapted from Petruzzelli and Iervolino (2021)

Following the evolution of design seismic actions, five sites, shown in Fig. 1 (right), were selected in the RINTC project to be representative of different hazard levels according to current standards and considering also the design epoch: Milan (MI), Rome (RM), Naples (NA), Catania (CT), L'Aquila (AQ).

3. Structural Typologies

3.1. Unreinforced Masonry Buildings

The residential URM buildings considered belong to two categories defined on the basis of the construction materials and technology adopted for walls and floor diaphragms: (i) *historical* (e.g. stone or brick masonry for walls and vaults or timber floors), and (ii) *modern* (e.g. with artificial block masonry for walls and reinforced concrete floors). These buildings are located at all the five sites considered in the project and some of them are also (ideally) seismically upgraded according to two codes: (a) the code enforced in Italy in 1981 (see Evolution of design codes section) and (b) the current Italian code (i.e. NTC18). The former code only allowed, as retrofitting, cementitious mortar injections and steel-reinforced plaster, with a structural analysis method involving nonlinear static analysis, based on the assumption of story-mechanisms with rigid diaphragms (i.e. the POR method; Tomažević 1978). The assessment according to the latter (current) code is instead based on pushover analysis of equivalent frame models. The evolution of design and construction for URM buildings is considered as follows: Pre-'20, '20-'45, '45-'87, Post-'87. More specifically, four Pre-'20 real case-study buildings were considered as located in Rome, Naples, Catania and L'Aquila. Four buildings, located in Milan and L'Aquila, are from the '20-'45 era and two in Catania and Milan are from the post *World-War-Two* period. Two buildings in Rome, from the Post-'87 era of the last century, are also considered and analyzed in their original state. Two buildings in Naples, were seismically upgraded (ideally) with both the code from the '80s and the current code, whereas two different buildings in L'Aquila were seismically upgraded both according to POR method and according to the current code.² Finally, a seven-story building in Rome was also upgraded according to the current code and analyzed in as per the retrofit conditions. Table 1 summarizes the considered cases, while Fig. 2 provides example of the

Table 1. Summary of the URM buildings considered in the project.

Design	Age	Site	Diaphragms	Masonry	Stores
Original	Pre-'20	Naples	Timber	Tuff stone	5
		Catania	Vaults	Lavic stone	3
		L'Aquila	Timber/Vaults	Undressed stone, clay brick (internal walls)	3
		Rome	Brick vaults/Mixed steel beams and brick thin vaults	Tuff stone and clay brick courses	7
	'20-'45	Milan	Reinforced concrete	Clay brick masonry	4
		L'Aquila	Timber	Undressed stone	2 and 3
	'45-'87	L'Aquila	Reinforced concrete	Undressed stone/Brick clay	3
Catania		Reinforced concrete (RC staircase)	Lavic stone	5	
Milan		Reinforced concrete	Horizontally perforated clay blocks	4	
Post-'87	Rome	Reinforced concrete	Vertically perforated clay bricks	2 and 3	
Seismically upgraded with '80s code	Pre-'20	Naples	Timber	Tuff stone	4 and 5
		Rome	Brick vaults/Mixed steel beams and brick thin vaults	Tuff stone with local strengthening and tie-rods	7
	'20-'45	L'Aquila	Reinforced concrete	Undressed stone with RC jacketing	2 and 3
Seismically upgraded with the current code	Pre-'20	Naples	Timber	Tuff stone	4 and 5
	'20-'45	L'Aquila	Timber with in-plane stiffening	Undressed stone with mortar injections and FRP	2 and 3

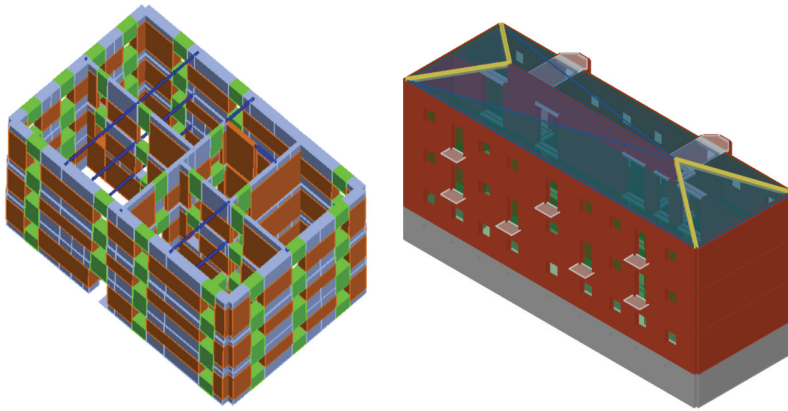


Figure 2. Example of a historical building in L'Aquila (left), and a modern one in Milan (right).

models for one historical and one modern buildings. The interested reader should refer to Penna, Rota, and Bracchi et al. (2022) and Lagomarsino, Cattari, and Angiolilli et al. (2022) for further details on the buildings and their design, modelling and analysis.

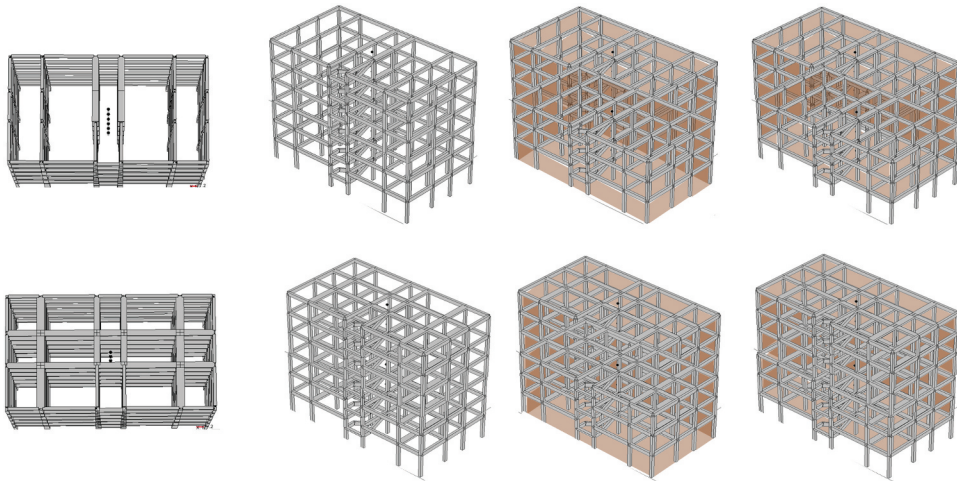
3.2. Reinforced Concrete Buildings

Reinforced concrete buildings are meant to be representative of the existing residential RC building stock in Italy, which mostly refers to post World War Two construction. Specifically, three and six story moment-resisting frames were considered. Gravity (RC-G), as well as seismic load design (RC-S), was considered with reference to three design epochs: '50-'60 (later denoted as Pre-'70), '70s and '80-'90, as in early 2000s the current code was established. These structures were defined through a simulated design process for the considered sites, which correspond to different seismic hazards; see the section 2.1. Gravity-load-designed buildings were designed according to different standards. Through the epochs the gravity loads did not change; however, design material properties and structural schemes evolved. Buildings featuring seismic design were assumed to be located in L'Aquila and Catania (II seismic category at the time of design, the most representative for the country), and thereby they were designed with a base shear equal to 0.07 times the building weight. This load did not change through the epochs, however, smooth rebars were abandoned in the '70s (whereas they were used in '50s & '60s). In the oldest buildings, seismic forces were applied to frames based on tributary areas, which corresponds to model the floors as (infinitely) flexible, and the moment-resisting internal frames were deployed in one horizontal direction only, with design forces only differing through the storeys because of the storey masses in a static analysis framework. This also characterizes the '70s buildings; however, the forces on the plane frames were based on their stiffness. In '80-'90, frames were deployed in two horizontal directions and a triangular acceleration distribution was assumed. For all buildings of all design eras, the allowable stress design method was used.

Modelling and analysis considered bare frames (BF), infilled (IF), and *pilotis* (PF) frame structures. IF and PF are characterized by a double-layer of bricks (12 + 8 cm and 15 + 8 cm for up to '70s and '80-'90 respectively). Details are given in De Risi, Di Domenico, and Terrenzi et al. (2022) for BF and Di Domenico, De Risi, and Manfredi et al. (2022) for IF and PF. Table 2 summarizes the considered cases, while Fig. 3 provides an example of six-storey RC buildings for the two extreme design epochs.

Table 2. Summary of the RC buildings cases.

Design	Epoch	Sites	Models	Storeys
Gravity loads	Pre-'70	Milan, Naples, Catania	BF,IF,PF	3,6
	'70s	Milan, Naples, Catania	BF,IF,PF	3,6
	'80-'90	Milan, Naples	BF,IF,PF	3,6
Seismic loads	Pre-'70	L'Aquila	BF,IF,PF	3,6
	'70s	L'Aquila	BF,IF,PF	3,6
	'80-'90	L'Aquila, Catania	BF,IF,PF	3,6

**Figure 3.** Top row: Pre-'70 BF, PF and IF structures (frames in one direction only). Bottom row: '80-'90 BF, PF and IF structures (frames in both directions with flat beams).

3.3. Precast Reinforced Concrete Buildings

The industrial precast reinforced concrete buildings are based on four case studies of real buildings in Italy, two from the '70s (denoted as EE1 and EE3), and two from the '80-'90 (denoted as EE2 and EE4). These buildings are all designed without accounting for seismic loads and according to allowable stress design. The two older buildings feature reinforced concrete infilled frames (bare frames are also modelled and analysed) and, as far as the roof is concerned, have a reinforced concrete topping that enables the rigid diaphragm; the beam-column connections are based on pure friction. The two most recent buildings do not have the reinforced concrete slab on the roof structure; EE2 has friction connections while the external cladding panels are precast both horizontally and vertically oriented (depending on which façade they cover). The EE4 building has dowel connections and horizontal external cladding panels. Differently from the older buildings, (both EE2 and EE4 have an offset between the cladding panels and the columns). These four buildings were considered located at Milan. Two of them (the oldest ones) were also relocated in Naples, while for the other buildings the details were re-designed for (newer, yet old with respect to current standards) seismic loads at the considered location. Finally, all of them were also re-designed for seismic loads in L'Aquila with the standards of the corresponding age and one of them (EE1) was re-designed with Pre-'70 standards; see Table 3. Details are given in Bosio, Di Salvatore, and Bellotti et al. (2022) while Fig. 4 provides a three-dimensional view of the typical PRC building model considered in the project.

Table 3. Investigated cases for PRC buildings.

Design	Epoch	Site	Roof	Cladding	Connections	
Gravity	'70s	Milan and Naples	Precast elements with additional RC topping	Infilled frames	Friction	
		Milan and Naples	Precast elements (wing-shaped)	Infilled frames	Friction	
	'80-'90	Milan	Precast elements with additional RC topping	Precast cladding panels	Friction	
Seismic	Pre-'70	L'Aquila	Precast elements (wing-shaped)	Precast cladding panels	Dowels	
		L'Aquila	Precast elements with additional RC topping	Infilled frames	Dowels	
	'70s	L'Aquila	Precast elements with additional RC topping	Infilled frames	Dowels	
			Precast elements (wing-shaped)	Infilled frames	Friction	
		'80-'90	Naples and L'Aquila	Precast elements with additional RC topping	Precast cladding panels	Dowels
				Precast elements (wing-shaped)	Precast cladding panels	Dowels

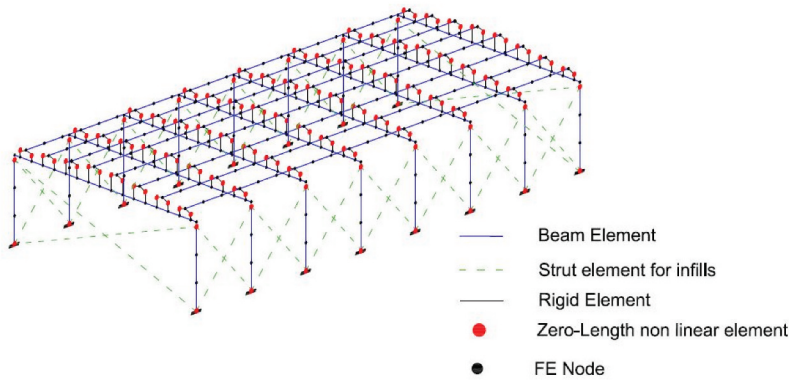


Figure 4. Industrial PRC buildings finite element (FE) model scheme.

3.4. Steel Buildings

The steel industrial building structures were obtained by simulating a design carried out according to the code and standards for steel buildings enforced in the years '80-'90 in Italy.³ The structures were considered placed at three sites, varying the structural configuration, but maintaining the same geometry, one 30 m bay in the transverse direction and four 8 m bays in the longitudinal direction. The height was about 9 m. Two schemes were adopted in the transverse direction: (i) hinged frame (PCB) and (ii) fully restrained frame (SCB). In the longitudinal direction bracing was placed in some portals, considering two cross sections: (a) L-shaped (L), and (b) square hollow section (SHS). The design for this kind of structures was carried out, according to the standards of the assumed time of construction, via admissible stresses on simplified structural schemes, for which linear analysis was applied. Design was driven by vertical and wind loads. For each structural configuration three cladding typologies were considered: (i) bare frame (BF); (ii) trapezoidal sheeting cladding (TS); (iii) sandwich panels sheeting (SP). Details are given in Cantisani and Della Corte (2022). Table 4 summarizes the considered cases, while Fig. 5 provides a three-dimensional view of the typical steel building designed, modeled, and analyzed in the project.

Table 4. Summary of steel-building cases.

Transverse scheme	Epoch	Sites	Geometry	Bracing	Cladding
PCB	'80-'90	Milan, Naples, L'Aquila	30 m x 8 m x 9 m	SHS	BF – TS – SP
		L'Aquila		L	BF – TS – SP
SCB	'80-'90	L'Aquila	30 m x 8 m x 9 m	SHS	BF – TS – SP
		L'Aquila		L	BF – TS – SP
		Milan, Naples			SP

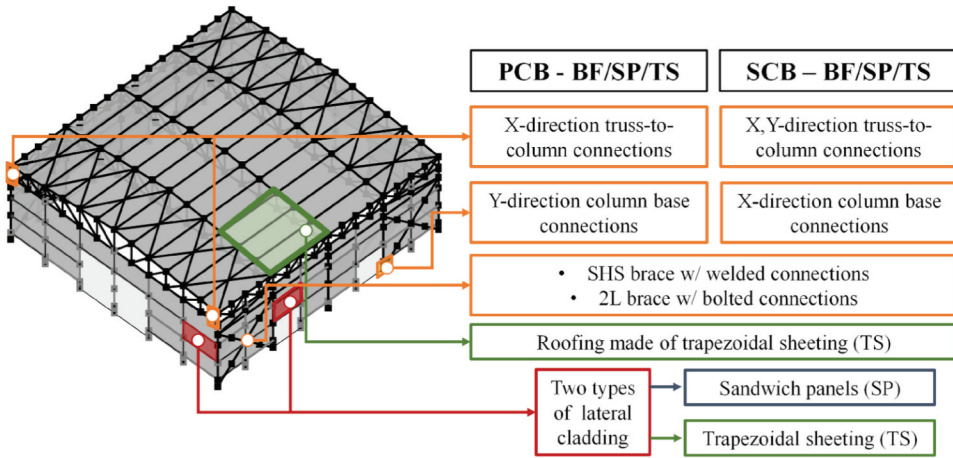


Figure 5. Steel building structure with cladding.

3.5. Base-isolated Buildings

For the case of BI, the objective was not to design the isolation system according to old codes, yet to protect the existing buildings designing the isolation system according to the current code, that is, NTC08/NTC18. In particular, for the existing fixed-base RC building (see Table 5), the base shear associated with the onset of plastic deformations was first identified by means of pushover analysis, assuming a uniform distribution of lateral forces. Then, the lowest value of the fundamental period of the base isolated building was derived entering the design spectrum with the spectral acceleration associated to the occurrence of the first plastic hinge. Next, the maximum displacement of the isolation system was evaluated using the displacement (code) spectrum at the *collapse-prevention* limit-state. Based on the target period and required displacement capacity, suitable devices were selected from the manufacturers' catalogues considering two isolation systems: (i) friction pendulums (FPS); (ii) high-damping rubber bearings and sliders (HDRB+S). The design verification of the base-isolated building was carried out through response spectrum analysis of a three-dimensional model of the structure, considering the performance requirements and compliance criteria specified in the current code; see Cardone, Viggiani, and Perrone et al. (2022), Micozzi, Flora, and Viggiani et al. (2021), and Ragni et al. (2018).

4. Failure Criteria

The seismic performance of all the described structures was assessed by running nonlinear dynamic analysis on numerical structural models. Structural reliability was assessed with respect to the exceedance of two damage states, global collapse (GC), and usability-preventing damage (UPD).

Table 5. Cases of base-isolated existing RC buildings.

Design	Epoch	Site	Storeys	Isolation system
Gravity loads	Pre-'70	Naples	6	FPS, HDRB+S
	'70s	Naples	6	FPS, HDRB+S
	'80-'90	Naples	6	FPS, HDRB+S
Seismic loads	Pre-'70	L'Aquila	6	FPS, HDRB+S
	'70s	L'Aquila	6	FPS, HDRB+S
	'80-'90	L'Aquila	6	FPS, HDRB+S

The GC criterion was, in general, defined based on the displacement capacity (i.e. roof drift RD or maximum interstorey drift ratio, MIDR, to follow) corresponding to the 50% drop of the maximum base-shear on the static pushover (SPO) curves of the structures for each horizontal direction. This is the case of the URM (with further limit states to consider additional local mechanism which will be introduced in the specific subsection), RC, S, and BI (for the superstructure) buildings. However, some adjustments and clarifications are required for some structural typologies. For URM buildings, the reference capacity thresholds are defined by SPO carried out in the two perpendicular (main) directions of the building, considering different load patterns (mass-proportional and triangular) in both positive and negative direction. For RC structures, the failure in terms of axial load carrying capacity for at least of one of the columns (in absence of redistribution capacity) is considered as an additional criterion. Regarding PRC buildings, GC occurs when: (i) one of the columns reaches its chord rotation capacity (which always occurs before the 50% maximum shear reduction); (ii) the friction connection fails (the main beams or the roof beams lose support); (iii) the dowel connection fails. For steel structures, joints failure was also considered, but in the analyses always occurred after the 50% drop condition.⁴ For BI structures, the failure of the base isolation system was defined based on the device-specific criteria. FPS system fails when a maximum displacement is reached; it is beyond the nominal capacity of the device and depends on: (i) exceeding a threshold of compression stress in the sliding interfaces equal to 60MPa ; (ii) half of the size of the slider itself (in fact, the first criterion dominates the results shown in the following). HDRB system fails when one of the following conditions occurs: (i) exceedance of 350% shear strain; (ii) numerical instability incoming with the attainment of a buckling load; (iii) traction axial deformation larger than 50%.

UPD follows a multi-criteria approach that needs to be specified for each structural typology. For the RC (and BI) structures, the criterion for BF structures is the onset of 0.5% interstorey drift, while in the IF and PF is onset of one of the following three: (i) reaching of 95% of maximum base shear (i.e. representative of a damage level not yet engaging a failure mechanism); (ii) severe damage in one infilling panel, where at least one infill with not-economically-feasible repair is present, (iii); light damage in at least 50% of all infillings. Both criteria can be considered tentatively coherent with what done for code conforming structures; see Iervolino, Spillatura, and Bazzurro (2018). For PRC structures, the failure for infillings criterion is the same as RC; moreover, failure of the connection of the cladding panels was considered as the onset of UPD; finally, 10% of the connection displacement capacity was considered as the onset of UPD (i.e. a damage level that can cause damage to roof finishing causing rain to drop in the building or to cascading damages to services connected to the roof elements). For steel structures, the criteria used for current-code-conforming buildings, are assumed: (i) reaching of the 95% of maximum base shear; (ii) severe damage in one non-structural element; (iii) light damage in more than 50% of the nonstructural elements. For URM structures, the attainment of the limit state was verified by implementing an approach coherent with the multi-criteria one just mentioned, considering as a response measure the MIDR (compared with reference thresholds defined by pushover analyses considering a triangular load pattern) or directly processing the information on damage from nonlinear dynamic analysis. The UPD attainment was identified by the first occurring among: (i) 50% of masonry piers reach the condition of light/moderate damage; (ii) one masonry pier reaches a severe damage condition; (iii) the base shear has reached the 95% of the peak resistance. (In any case, the final threshold should correspond to a value of the base shear not lower than the 85% of the peak resistance; to prevent UPD from occurring with a widespread damage but still far from the maximum strength.)

4.1. Historical URM Buildings

Historical URM buildings are vulnerable to local mechanisms that are not explicitly modelled in the three-dimensional global model of the building, but should be taken into account in the evaluation of both GC and UPD. In particular, the local mechanisms considered herein are:

- detachment and overturning of the upper portion of the façade: out-of-plane response of local mechanisms is evaluated by nonlinear dynamic analyses on single degree of freedom models, by applying the acceleration time history obtained from the global model at the location where rocking might occur; two performance levels are considered: *local collapse* (LC) and *severe damage* (SD). The former is attained when the maximum displacement from the NLDA is greater or equal to 95% of the displacement corresponding to the static limit equilibrium of the overturning façade, while the latter refers to a condition (40% of the static limit equilibrium) that is far from overturning but is usually associated to permanent rotation;
- damage and collapse of brittle horizontal diaphragms (masonry vaults, lightened floors without continuous reinforced concrete slabs). Two performance levels are considered: *local collapse* (LC) and *severe damage* (SD); the former is attained when vaults suffer very severe cracks and have lost the original shape, while lightened floors suffer crumbling of the hollow bricks. The latter refers to severe cracks; for each diaphragm, the maximum horizontal in-plane drift is evaluated from the displacement time history obtained from the global model and compared to specific horizontal drift thresholds; the limit state is attained when 50% of the horizontal diaphragms has reached the corresponding drift threshold.

The local mechanisms contribute to the failure criteria as follows: LC criteria concur to assess the onset of GC along with those already defined, while the SD criteria are added to those defining UPD.

5. Methodology

5.1. Sites' Hazard

Seismic reliability assessment, in this study, relied on nonlinear dynamic multi-stripe analysis (MSA, Jalayer and Cornell 2009, see next section) carried out on three-dimensional structural models subject to pairs of horizontally recorded ground motions. The records were selected in hazard-consistent manner (to follow); therefore, the computation of probabilistic seismic hazard curves for the five sites under investigation is a preliminary and essential step. All the curves were computed using, as the ground motion intensity measure (*IM*), the pseudo-spectral acceleration (5% damped), S_a , at vibration periods, T , close to the first-mode vibration periods of the examined structural models, mostly for soil condition C and in two cases for soil condition A (according to the soil classification of CS.LL.PP. 2018). Table 6 summarizes the hazard analysis performed and the corresponding *IMs*.

Hazard curves, expressed in terms of annual exceedance rate (λ_{im}) of *IM* thresholds (*im*), were first computed using the seismic zone source model for Italy of Meletti et al. (2008), with the magnitude distribution and rates described in Barani, Spallarossa, and Bazzurro (2009), and the ground motion prediction equation of Ambraseys, Simpson, and Bommer (1996), or that of Akkar and Bommer (2010) for periods beyond 2s. Hazard analysis was carried out via REASSESS software (Chioccarelli

Table 6. Sites and spectral ordinates where hazard curves were computed (identified by the symbol \checkmark).

Site	$S_a(0.15s)$		$S_a(0.25s)$		$S_a(0.5s)$		$S_a(1s)$		$S_a(2s)$		$S_a(3s)$	
	A	C	A	C	A	C	A	C	A	C	A	C
L'Aquila (AQ)	\checkmark	-	-	-	-	\checkmark	-	\checkmark	-	\checkmark	-	\checkmark
Catania (CT)	-	-	-	-	-	\checkmark	-	\checkmark	-	-	-	-
Naples (NA)	-	-	-	\checkmark	-	\checkmark	-	\checkmark	-	\checkmark	-	\checkmark
Rome (RM)	-	\checkmark	-	-	-	\checkmark	-	-	-	-	-	-
Milan (MI)	\checkmark	\checkmark	-	-	-	\checkmark	-	\checkmark	-	\checkmark	-	\checkmark

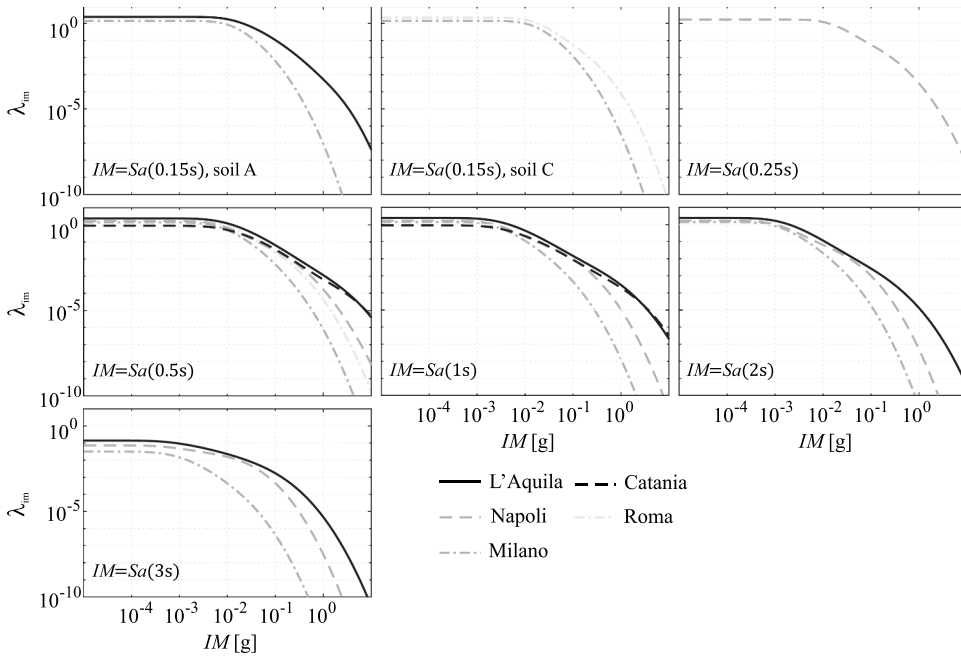


Figure 6. Hazard curves for all the IM used in the project.

et al. 2019). The seismic source model used for the hazard assessment is coherent with the one employed by the Italian code to define the design seismic actions on structures; that is, Stucchi et al. (2011). The resulting hazard curves thus evaluated are shown in Fig 6.⁵

5.2. Record Selection

Seismic fragility of the designed structures was assessed by subjecting the models to MSA that, like incremental dynamic analysis (IDA, Vamvatsikos and Cornell 2002), has the objective of determining a relationship between the *engineering demand parameter (EDP)* and *IM* for the structural model analysed. However, differently from IDA, it may use different sets of records at each *IM*-level, to be consistent with the site-specific hazard characteristics. For the purposes of this study, record selection was carried out according to the procedure by Spillatura et al. (2021), in which the selected time histories are hazard consistent in terms of spectral shape and also of the main parameters of the most likely causative events; that is, earthquake magnitude, *M*, and source-to-site distance, *R*, from hazard disaggregation (e.g. Iervolino, Chioccarelli, and Convertito 2011). This procedure is considered an enhancement of the *conditional spectrum (CS)* method of Lin, Haselton, and Baker (2013) and, for each site and each first-mode vibration period of interest, *T1*, can be summarized as follows:

- (a) compute hazard disaggregation conditional on $Sa(T1) = sa_i$, where sa_i corresponds to each one of the considered 10 values with exceedance return periods, T_R , ranging from 10 to 100000 years at the site;
- (b) build, for each sa_i value, the corresponding CS distribution⁶;
- (c) simulate 20 response spectra consistent with the CS distribution from the previous step;
- (d) select 20 real ground motion records having spectra compatible with those simulated;

- (e) post-process the selected set, eventually replacing the records that are not disaggregation-consistent with other spectrally equivalent ground motions with desired M and R from disaggregation.

As an example, Fig. 7 shows the 10 conditional spectra (mean and two percentiles) for the 10 IM stripes considered for L'Aquila (left) and Milan (right) sites (soil C class), when the IM is $Sa(1s)$. Conditional spectra (mean and two percentiles) referring to the L'Aquila (left) and Milan (right) sites for soil C class, when the conditioning IM is $Sa(1s)$.

Hence, the record selection procedure delivered 200 pairs of records for each IM , 20 records for each one of the ten stripes. The records selected with this procedure were extracted mainly from the *Italian accelerometric archive* (<http://itaca.mi.ingv.it/>; Luzi et al. 2008) and only when no records with suitable spectral shape were available within this dataset, the algorithm searched in the *NGAwest2* database (<http://peer.berkeley.edu/ngawest2/>; Ancheta et al. 2014) instead. To reduce the computational demand of nonlinear dynamic analysis, the selected records have been post processed to remove the parts of the signal outside the $[t_{0.05\%}; t_{99.95\%}]$ range, where $D_{99.90\%} = t_{99.95\%} - t_{0.05\%}$ is the 99.90% significant duration of the record (Dobry, Idriss, and Ng 1978), yet keeping synchronization of horizontal components.

5.3. Reliability Assessment

In the project, the three-dimensional numerical models for structural analysis were built in OPENSEES (McKenna et al. 2000) except for URM buildings that were analyzed using TREMURI (Lagomarsino et al. 2013). The output of the analysis, for each building, consists of 10 stripes of 20 structural responses each obtained from the simultaneous application of pairs of horizontal accelerograms for the two horizontal directions of the structural models along which structural members are aligned. As discussed in the previous section, the response measure considered is either the MIDR or RD. However, to identify failure for both performance levels (GC and UPD), the maximum demand-over-capacity ratio among the two directions can be considered; therefore, such a ratio is the actual EDP considered in the reliability assessment and $EDP \geq 1$ identifies failure. In the numerical analysis, there were also some cases of numerical instability, according to the definition of Shome and Cornell (2000), which leads directly to certain failure.⁷ Fig. 8a provide an example of records selected for

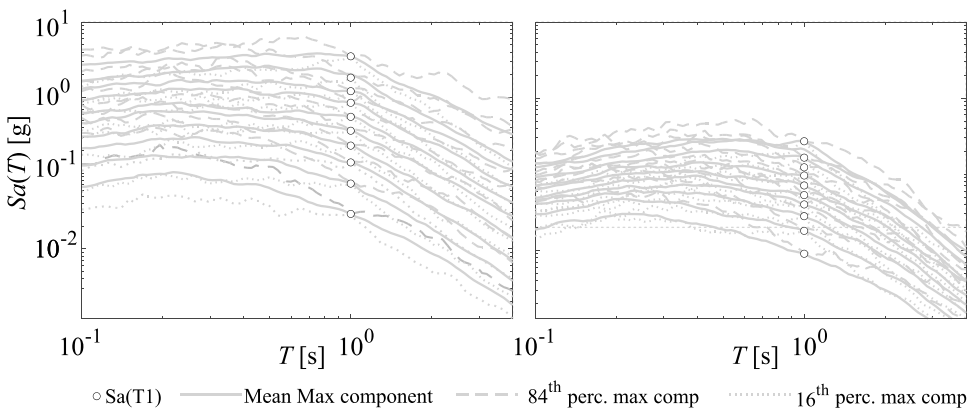


Figure 7. Conditional spectra (mean and two percentiles) referring to the L'Aquila (left) and Milan (right) sites for soil C class, when the conditioning IM is $Sa(1s)$.

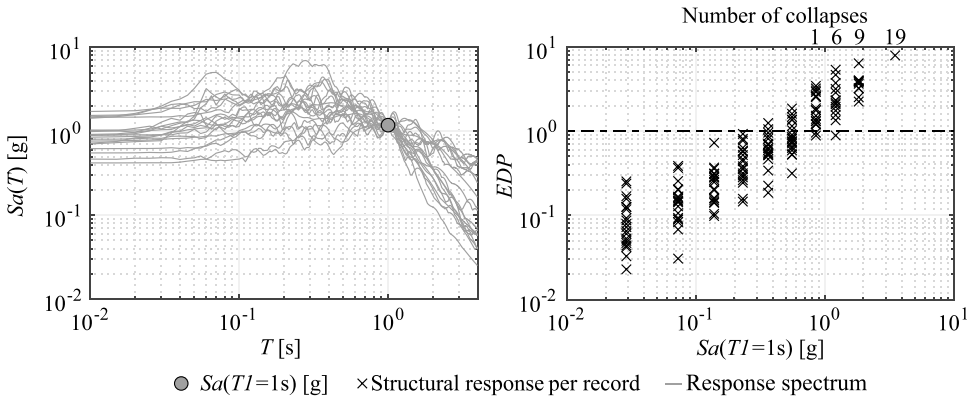


Figure 8. Example of hazard-consistent record-selection for MSA (left); example of MSA results when the EDP is the demand-to-capacity ratio (right).

L’Aquila, soil condition C, when the IM is Sa(1s) corresponding to $T_R = 5000yr$ at the site; while Fig. 8b gives the result of the analysis at 10 stripes for the RC structure identified as RC_3_’70s_IF_C_AQ (see Appendix).

The metric taken for the seismic reliability is the rate of earthquakes causing failure of the structure, λ_f , which can be calculated as:

$$\lambda_f = \int_{IM} P[f|IM = im] \cdot |d\lambda_{im}| \approx \int_0^{IM_{T_R=10^5}} P[f|IM = im] \cdot |d\lambda_{im}| + 10^{-5} \quad (1)$$

where $P[f|IM = im]$ is the fragility of the structural model, that is the probability of failure (i.e. GC or exceedance of UPD), conditional to $IM = im$ and $|d\lambda_{im}|$ is the absolute value of the derivative of the site-specific hazard curve times $d(im)$. Structural failure was considered to have been reached in cases of numerical instability or the attainment of the collapse criteria in either of the two horizontal directions. Given that collapse is indicated as C, fragility has been evaluated via an application of the total probability theorem:

$$P[f|IM = im] = P[C|IM = im] + P[EDP \geq 1|\bar{C}, IM = im] \cdot \{1 - P[C|IM = im]\} \quad (2)$$

where $P[EDP \geq 1|\bar{C}, IM = im]$ and $P[C|IM = im]$ are, given IM, the probability of failure given non-collapse and collapse, respectively.

It was mentioned above that site-specific hazard curves within RINTC project have been evaluated for 10 return periods T_R with an upper bound equal to 100000yr so a full evaluation of the failure rate is prevented. Consequently, it has been conservatively assumed that ground-motions having IM larger than the IM corresponding to $T_R = 100000yr$ named $IM_{T_R,max}$, will certainly cause structural failure, as shown in the last equality of equation (1), where 10^{-5} is added to the integral to account for the truncation of the hazard curve at $\lambda_{im} = 10^{-5}$. The discretization of the structural analysis at the 10 IM levels and the use of 20 pairs of ground motions at each IM stripe yielded the following approximation in computing equations (1) and (2):

$$\lambda_{im} = 10^{-5} \quad (3)$$

In the equation $\Phi(\cdot)$ is the cumulative Gaussian distribution function and N_{C,im_i} is the number of numerical instabilities at the im_i stripe.

6. Results and Discussion

6.1. Pre- and low-code Reliability Comparison with new-design

Figure 9, for GC and UPD, reports the failure rates computed according to equation (1), where the fragility of the building is evaluated with equations (2) and (3), that is, without fitting a fragility curve thought the MSA results data. As discussed, this is the same approach for current-code-conforming structures adopted in Iervolino, Spillatura, and Bazzurro (2018) and allows a direct comparison with seismic reliability computed in there, at least for the sites that both studies share; that is, Milan, Naples, and L'Aquila. In order to facilitate the comparison, both the results for current-code-conforming structures and existing structures, are reported in the figures. It should be specified that several current-code-conforming structures belonging to the five structural typologies were designed for the two soil conditions A and C, whereas structures herein designed are mainly located on soil C for all the typologies except for some URM building located on soil A. The data in the figures are organized as a function of the (grossly) decreasing hazard of the sites from left to right, defined based on the hazard curves (e.g. Fig. 6); the results show that the seismic reliability tends to decrease as a function of increasing hazard. Moreover, the computed reliability at the least hazardous site, that is, Milan, is below 10^{-5} , and therefore, according to equation (3), this value is assumed as the failure rate. This lower bound of reliability also applies to selected structural typologies at some sites that can be considered as characterized by mid-hazard (see also Fig. 1, right). Finally, the UPD rates tend to be larger, in general, by orders of magnitude, with respect to those referring to GC. It is also noted that URM appears to be the least reliable typology. These conclusions are similar to what found for current-code-conforming buildings and are expected to be driven to the same factors. On the other hand, in general, the figure shows that the seismic reliability of pre- or low-code structures tends to be lower for structures of the same typology at the same site. This is something that preliminarily confirms the improvement of codes, as they evolve in time.

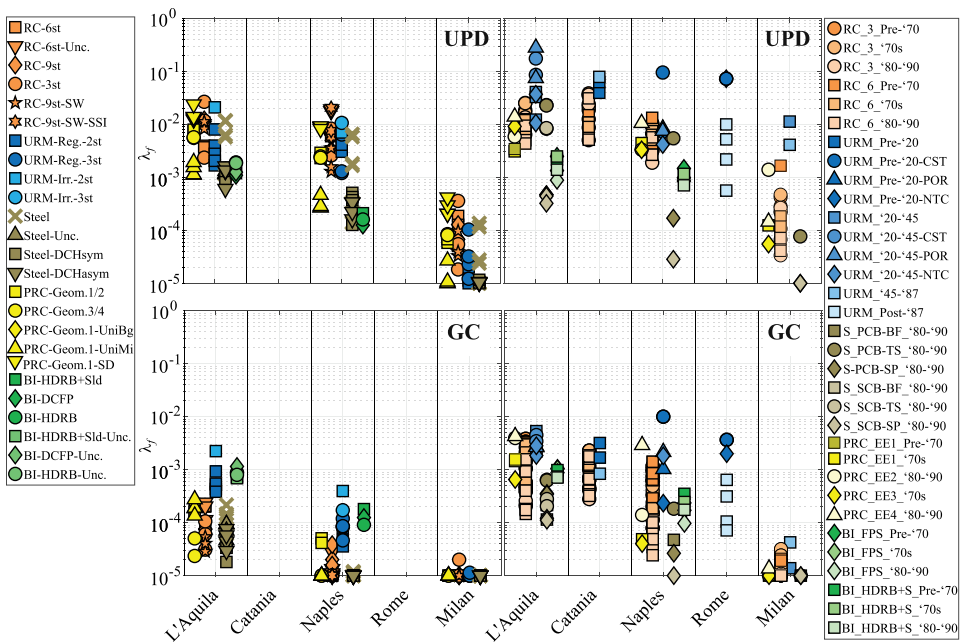


Figure 9. UPD (upper panels) and GC (bottom panels) failure rates for buildings designed according to current design prescriptions (left side) and according to pre- and/or old-codes prescriptions (right side). IDs of new buildings are the same as in (Iervolino, Spillatura, and Bazzurro 2018), while those of existing buildings are specified in the Appendix.

The figures also allow to appreciate that the typology-to-typology variability of the failure rates tends to increase in the pre- and low-code case with respect to current-code-conforming buildings. Nevertheless, this comparison is always delicate, because although coherency in structural modelling and analysis was a precise goal of the RINTC project, the different characteristics of the typologies and of their failure modes, likely impedes in-depth comparability of the failure rates. It is believed that this issue, which also affects the results for current-code-conforming structures, is magnified in pre- and low-code structures because of the larger heterogeneity of their characteristics and seismic behavior.

6.2. Typological Evolution of Reliability in Time

In this section, the typological evolution of the seismic reliability as a function of the evolution of seismic codes is investigated; this is considered the main goal of the present study. For this analysis, the failure rates are computed via equation (1), yet using the lognormal parametric fragility curves fitted through MSA results for each structural model, which are given in the Appendix. This allows the integration of hazard and fragility in an *IM* domain extended beyond $T_R = 100000yr$. Each of the figures refers to a single typology. Fig. 10 for URM, Fig. 11 for RC-S, Fig. 12 for RC-G, Fig. 13 for PRC, Fig. 14 for S, and Fig. 15 for BI. The figures, in line with the previous sections, are organized in order to separate the different sites and also to identify, at each site, the design epoch (see Structural typologies section). To enhance the readability of the figures, and also to simplify the comparisons, the failure rates are not presented in terms of individual structures, but as simple arithmetic averages. Nevertheless, where applicable, bars representing the minimum-maximum variations of rates the mean refers to, are also given. All the figures include the corresponding average rates for code conforming structures calculated via parametric fragilities (Iervolino, Baraschino, and Cardone et al. 2021).

Analyzing the figures, it emerges that at GC, for all the typologies, the averages (and range of variation) of failure rates tends to be larger than those of current-code-conforming structures of the same typology at the same site. However, there are some exceptions. The PRC structure designed in L’Aquila in the ‘80s-‘90s seems to be less reliable than the older buildings, yet this is not strictly due to the evolution of codes rather to the different plan configurations and design choices previously described (as for the structures designed in Milan). At UPD, gravity-load-designed PF and IF, six storeys, RC-buildings sited in Milan, according to the prescriptions in force during the ‘70s seem to be less reliable than those designed with reference to the epochs pre-‘70s (‘50-‘60); this lower capacity is

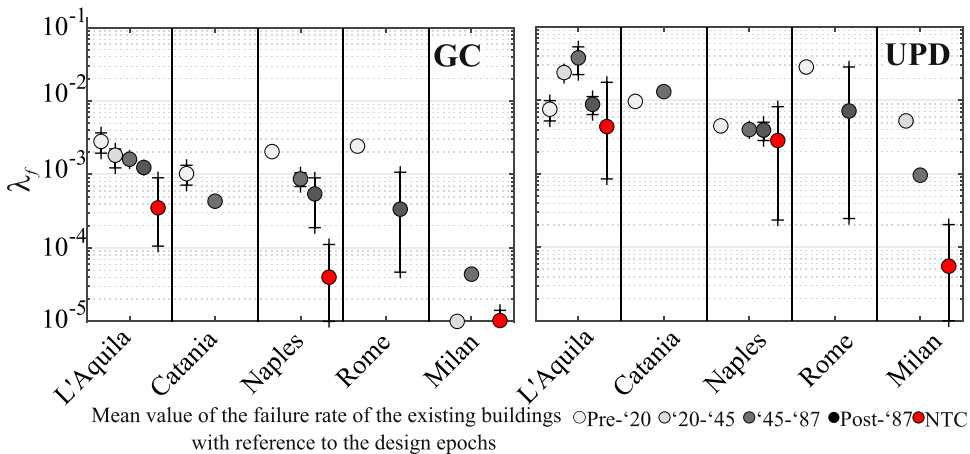


Figure 10. Arithmetic averages of the failure rates for all the existing URM structures at GC (left) and UPD (right).

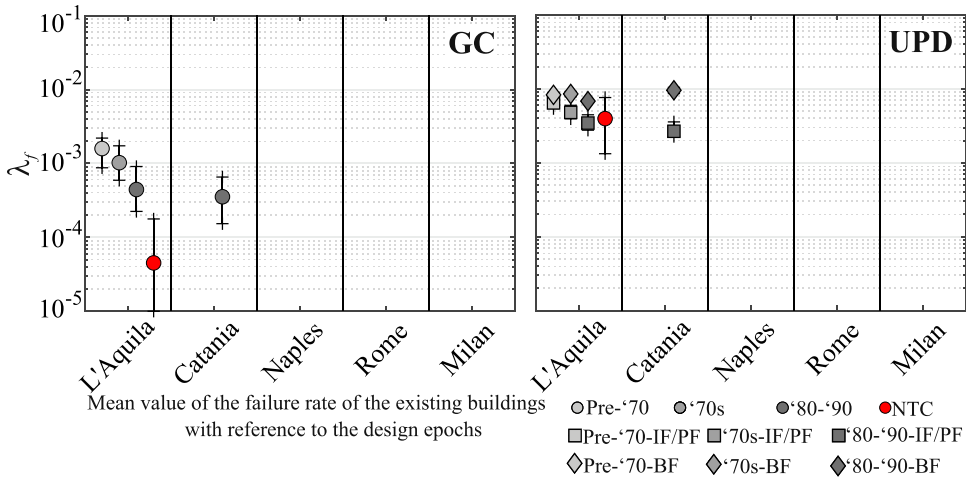


Figure 11. Arithmetic averages of the failure rates for all the existing RC-S structures at GC (left) and UPD (right).

due to shear failures observed in the former case-study building. This singularity occurs for all the RC buildings (i.e. both seismic- and gravity-load design) but the decreasing in capacity does not always result in an opposite trend of the failure rates; that is, for most RC buildings cases mean values of the failure rate are similar for the two mentioned epochs. Further discussions on these issues can be found in the typology-specific papers already cited.

The heterogeneity (i.e. variability range) of the results for the existing structures is mostly lower than that of new code-conforming buildings, but minimum failure rates are always larger than those of new constructions (at UPD the situation is less clear). However, such heterogeneity directly derives from the case study buildings, which are somewhat arbitrary. At UPD, as already mentioned, the URM buildings tends to be the least seismically reliable typology; that is, mean and maximum rates are larger than those assessed for the other typologies. This is even clearer for the buildings designed before the

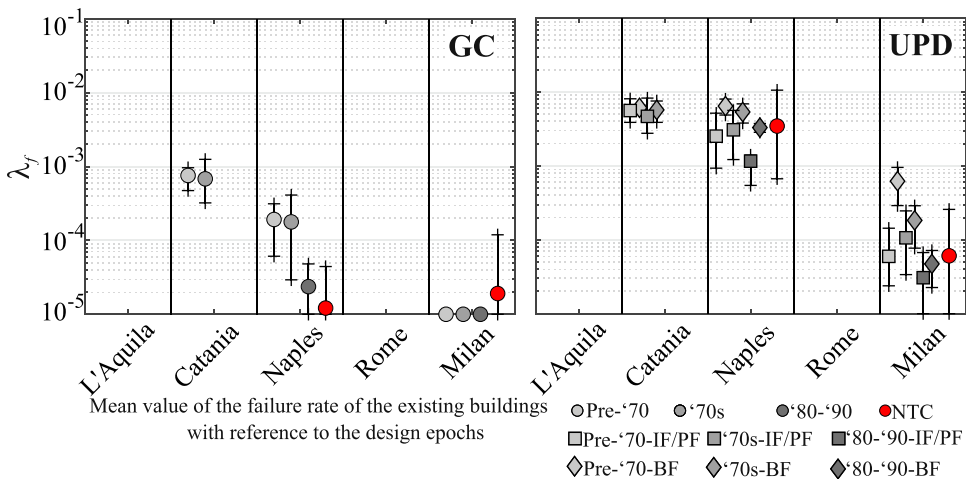


Figure 12. Arithmetic averages of the failure rates for all the existing RC-G structures at GC (left) and UPD (right).

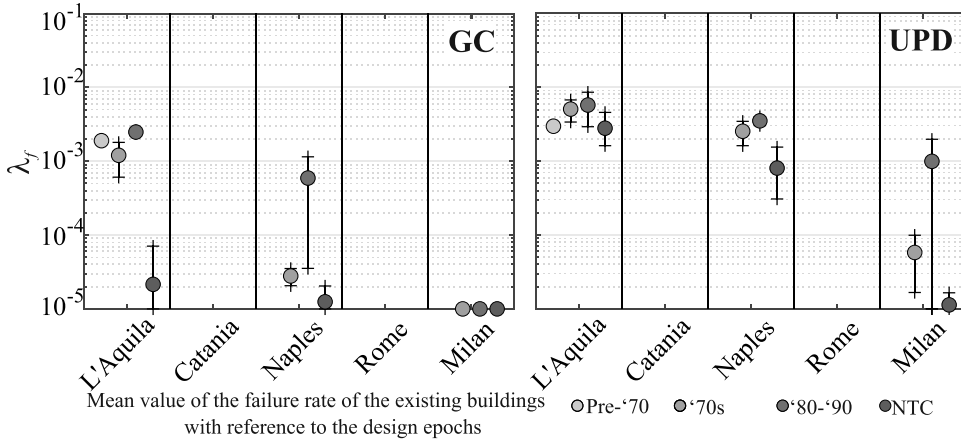


Figure 13. Arithmetic averages of the failure rates for all the existing PRC structures at GC (left) and UPD (right).

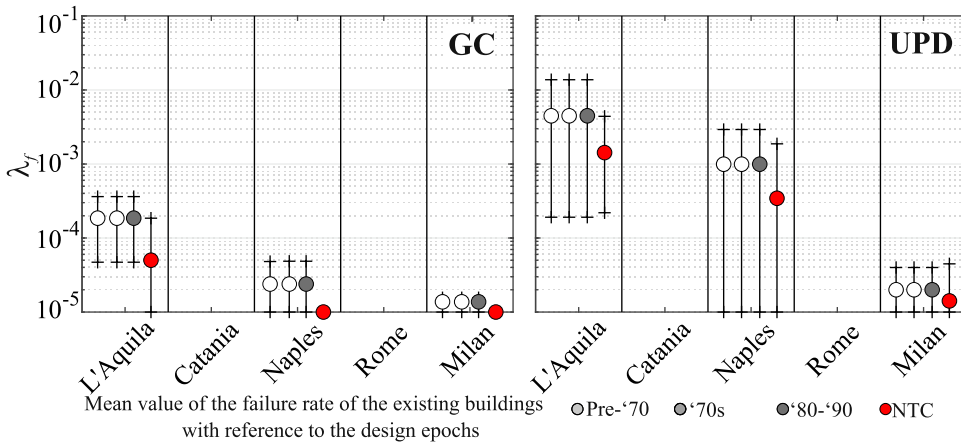


Figure 14. Arithmetic averages of the failure rates for all the existing S structures at GC (left) and UPD (right). White circles mean that the prescriptions for S structures designed in the '80-'90 also apply to previous epochs.

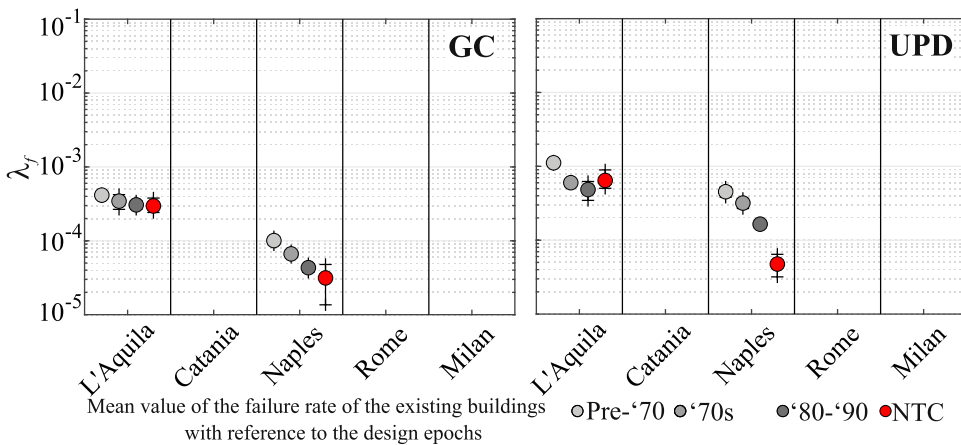


Figure 15. Arithmetic averages of the failure rates for all the existing BI structures at GC (left) and UPD (right).

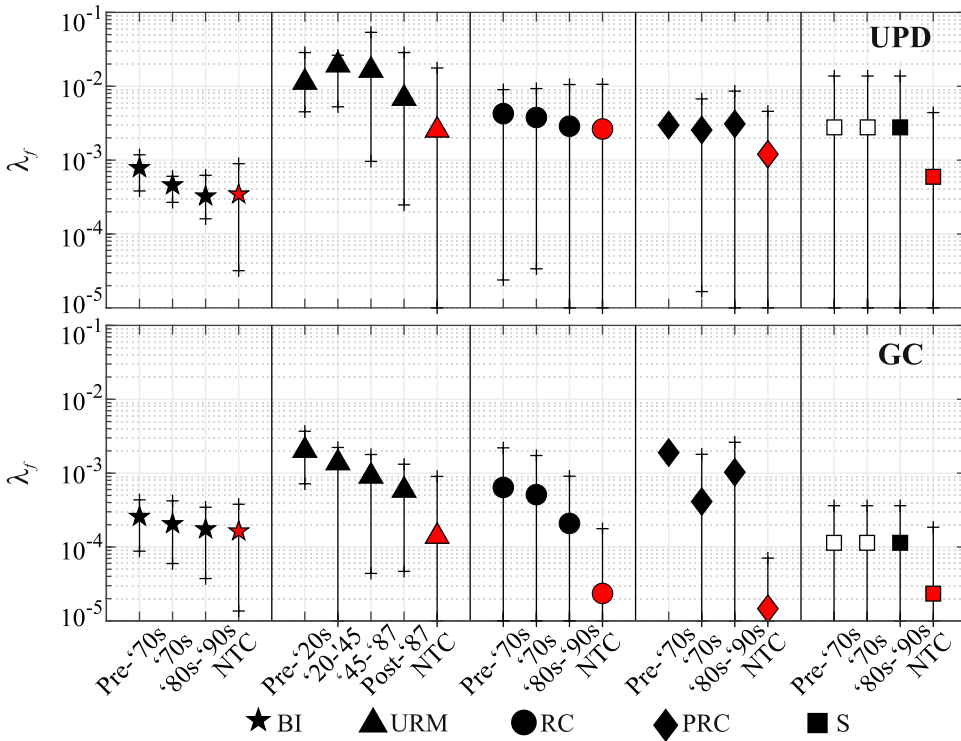


Figure 16. Arithmetic averages of the failure rates for all the existing structures at UPD (upper) and GC (bottom) as a function of the design epoch. White squares mean that the prescriptions for 5 structures designed in the '80-'90 also apply to previous epochs.

'90s. As final summary, Fig. 16 shows the average failure rates as a function of the design epoch pooling together the data from different sites. This representation further supports the remarks discussed in the previous lines.

7. Conclusions

This paper has presented and discussed the results of a large research program aimed at evaluating the seismic structural reliability of pre- and low-code-conforming buildings in Italy, referring to some common residential and industrial structural typologies, that is, fixed-base and base-isolated reinforced concrete, precast-reinforced concrete, unreinforced masonry, and steel. The buildings were designed (and/or retrofitted according) to major updates of building codes enforced in Italy in the last century. The design was carried out in five sites in Italy, characterized by different level of seismic hazard, evaluated by means of the PSHA on which the current design provisions are based. State-of-the art three-dimensional structural models were developed to run multi-stripe analysis performed with hazard-consistent record selection. The seismic reliability was measured in terms of annual rates of earthquakes causing failure, the latter defined in terms of two, ad-hoc defined, performances: global collapse (GC) and usability-preventing damage (UPD).

This work allowed to assess the typological evolution of the seismic structural reliability as a function of the design era (i.e. as the design codes evolved) and its comparison with that of current-code-conforming structures, which was addressed in a previous study that was methodologically consistent with this one. A few remarks can be finally drawn.

- The seismic reliability tends to decrease as the seismic hazard of the construction site increases. This is consistent with the findings of previous studies, developed following the same framework, and related to current-code-conforming buildings.
- For GC, the seismic reliability of pre- and low-code buildings is lower than that of structures designed according to the current code, although with some exceptions mainly due to design and modelling rationales.
- For UPD, the trend is less clear, possibly also because it is difficult to define UPD in a sufficiently coherent manner between pre- and low-code and current-code-conforming structures.

A side result of the study is the development, via state-of-the-procedures, of lognormal fragility curves for all structural models and for both GC and UPD performance levels. The obtained curves, provided in the Appendix, can be potentially used for further studies related to seismic risk of existing Italian buildings or to investigate the relative impact of various aspects of code evolution (e.g. changes in territorial classification and seismic actions vs enforcement of seismic design principles) on the seismic reliability.

Notes

1. A peculiar, yet relevant, aspect is that, between 1916 and 1936 or 1937 and 1962, several municipalities were *de-classified*, that is, taken from being classified as seismically prone zones to non-seismically-prone.
2. Eventually, retrofit interventions were assessed according to NTC18.
3. Though the numerical results are strictly referred to the investigated case study buildings and relevant design assumptions for the period '80-'90, it is contended that the results are essentially applicable, at least qualitatively, to buildings designed and built in Italy since the '60s and characterized by failure modes similar to the case studies investigated here.
4. Also, it is to note that for the current-code-conforming steel buildings (Scozzese et al. 2018) a (somewhat conservative) criterion to account for fracturing braces was considered. This was not necessary herein as post-fracture behavior was explicitly modelled.
5. In fact, while the hazard curves to select records were computed via OPENQUAKE (Monelli, Pagani, and Weatherill et al. 2012), the hazard curves to be integrated with structural fragility for reliability assessment, were re-computed via REASSESS software because integration with lognormal (i.e. parametric) fragility requires a much larger IM range, beyond $T_R = 100000yr$.
6. To compute the CS distribution a GMPE is required. For consistency with PSHA, the one from Ambraseys, Simpson, and Bommer (1996) has been used, which considers, as the IM , the maximum spectral acceleration between the two horizontal components. However, it is limited to spectral ordinates up to $Sa(T = 2s)$; therefore, when the vibration period of the conditioning spectral acceleration was larger than $2s$ (i.e. for BI structures) the Akkar and Bommer (2010) GMPE was considered instead. It considers, as the IM , the geometric mean of the two horizontal components so, for consistency, when the vibration period of the conditioning spectral acceleration is greater than $2s$ the CS matching was performed using the latter as IM .
7. The failure mechanisms that, for some typologies, have capacity which is not directly measured by MIDR or RD also lead to $EDP = 1$ in case of failure.
8. The acronym CST (current state) is used for the buildings later upgraded by means seismic codes prescriptions (NTC18 or POR).
9. Steel structures without cladding (BF) were not analysed at UPD.

Acknowledgments

The comments from Dr. Dimitrios Vamvatsikos (*National Technical University of Athens*, Greece), Dr. Matthew Fox (*Università degli Studi di Pavia*, Italy), and an anonymous reviewer, that have improved quality and readability of this paper, are gratefully acknowledged.

Disclosure Statement

No potential conflict of interest was reported by the author(s).

Funding

This work was supported by Centro Europeo di Formazione e Ricerca in Ingegneria Sismica [EUCENTRE-DPC2019–2021 research program] and Rete dei Laboratori Universitari di Ingegneria Sismica [ReLUIIS-DPC2019–2021 research program]. The opinions and conclusions presented by the authors do not necessarily reflect those of the funding entities.

ORCID

Iunio Iervolino  <http://orcid.org/0000-0002-4076-2718>
 Roberto Baraschino  <http://orcid.org/0000-0002-8363-9306>
 Andrea Spillatura  <http://orcid.org/0000-0002-4302-0955>

References

- Akkar, S., and J. J. Bommer. 2010. Empirical equations for the prediction of PGA, PGV, and spectral accelerations in Europe, the Mediterranean region, and the Middle East. *Seismological Research Letters* 81: 195–206. doi:10.1785/gssrl.81.2.195.
- Ambraseys, N. N., K. A. Simpson, and J. J. Bommer. 1996. Prediction of horizontal response spectra in Europe. *Earthquake Engineering & Structural Dynamics* 25: 371–400. doi:10.1002/(SICI)1096-9845(199604)25:4<371::AID-EQE550>3.0.CO;2-A.
- Ancheta, T. D., R. B. Darragh, J. P. Stewart, E. Seyhan, W. J. Silva, B. S.-J. Chiou, K. E. Wooddell, R. W. Graves, A. R. Kottke, D. M. Boore, et al. 2014. NGA-West2 database. *Earthquake Spectra* 30. doi:10.1193/070913EQS197M
- Angiolilli, M., M. Etete Minkada, M. Di Domenico, S.Cattari, A.Belleri, and G. M.Verderame. 2022. Comparing the observed and numerically simulated seismic damage: a unified procedure for unreinforced masonry and reinforced concrete buildings. *Journal of Earthquake Engineering* (in press)
- Baltzopoulos G, Grella A and Iervolino I. 2021. Seismic reliability implied by behavior-factor-based design. *Earthq Engng Struct Dyn*, 50(15): 4076–4096. doi:10.1002/eqe.3546
- Barani, S., D. Spallarossa, and P. Bazzurro. 2009. Disaggregation of probabilistic ground-motion Hazard in Italy. *Bulletin of the Seismological Society of America* 99: 2638–61. doi:10.1785/0120080348.
- Bosio M, et al. 2022. Modelling and Seismic Response Analysis of Non-residential Single-storey Existing Precast Buildings in Italy. *Journal of Earthquake Engineering*, 1–22. doi:10.1080/13632469.2022.2033364
- Cantisani, G., and G. Della Corte. 2022. Modelling and seismic response analysis of non-residential existing steel buildings in Italy. *Journal of Earthquake Engineering* 1–33. doi:10.1080/13632469.2022.2030438.
- Cardone D, et al. 2022. Modelling and Seismic Response Analysis of Existing Italian Residential RC Buildings Retrofitted by Seismic Isolation. *Journal of Earthquake Engineering*, 1–25. doi:10.1080/13632469.2022.2036271
- CEN. 2004. *EN 1998-1: Eurocode 8 - Design of structures for earthquake resistance. Part 1: General rules, seismic actions and rules for buildings*. Bruxelles, Belgium: European Committee for Standardization.
- Chioccarelli, E., P. Cito, I. Iervolino, and M. Giorgio. 2019. REASSESS V2.0: Software for single- and multi-site probabilistic seismic hazard analysis. *Bulletin of Earthquake Engineering* 17: 1769–93. doi:10.1007/s10518-018-00531-x.
- Cito, P., and I. Iervolino. 2020. Peak-over-threshold: Quantifying ground motion beyond design. *Earthquake Engineering & Structural Dynamics* 49: 458–78. doi:10.1002/eqe.3248.
- Cornell C Allin. 1968. Engineering seismic risk analysis. *Bulletin of the Seismological Society of America*, 58(5): 1583–1606. doi:10.1785/BSSA0580051583
- CS.LL.PP. 2008. Norme tecniche per le costruzioni. Gazz Uff della Repubb Ital 29. (in Italian)
- CS.LL.PP. 2018. Aggiornamento delle “Norme tecniche per le costruzioni.” Gazz Uff della Repubb Ital 42. (in Italian)
- De Risi M T, et al. 2022. Modelling and Seismic Response Analysis of Italian pre-code and low-code Reinforced Concrete Buildings. Part I: Bare Frames. *Journal of Earthquake Engineering*, 1–32. doi:10.1080/13632469.2022.2074919
- Decreto Ministeriale. 1975. Legge n°40 del 3 marzo 1975. Approvazione delle norme tecniche per le costruzioni in zone sismiche. Gazz Uff della Repubb Ital GU 93. (in Italian)
- Decreto Ministeriale. 1981. Legge n°515 del 4 giugno 1981. Classificazione sismica del territorio e basati su uno studio del CNR. Gazz Uff della Repubb Ital GU (in Italian)
- Decreto Ministeriale. 1984. Legge n°40 del 18 giugno 1984. Norme tecniche relative alle costruzioni smiche. Gazz Uff della Repubb Ital GU 208. (in Italian)
- Decreto Ministeriale. 1996. Norme tecniche per le costruzioni in zone sismiche. Gazz Uff della Repubb Ital GU 29. (in Italian)
- Di Domenico M, et al. (2022). Modelling and Seismic Response Analysis of Italian Pre-Code and Low-Code Reinforced Concrete Buildings. Part II: Infilled Frames. *Journal of Earthquake Engineering*, 1–31. doi:10.1080/13632469.2022.2086189

- Di Pasquale, G., A. Fralleone, A. G. Pizza, and C. Serra. 1999. Relevant changes to the Italian seismic Code from 1909 to 1975 – A synoptic table. *La Classif e la Norm sismica Ital dal 1909 al 1984*, Marco, R Martini, MG, Ist Poligr e Zecca dello Stato, Roma. (in Italian)
- Dobry, R., I. M. Idriss, and E. Ng. 1978. Duration characteristics of horizontal components of strong-motion earthquake records. *Bulletin of the Seismological Society of America* 68: 1487–520. doi:10.1785/BSSA0680051487.
- Fardis M N. (2018). Capacity design: Early history. *Earthquake Engng Struct Dyn*, 47(14), 2887–2896. doi:10.1002/eqe.3110
- Iervolino, I., E. Chioccarelli, and V. Convertito. 2011. Engineering design earthquakes from multimodal hazard disaggregation. *Soil Dynamics and Earthquake Engineering* 31: 1212–31. doi:10.1016/j.soildyn.2011.05.001.
- Iervolino, I., M. Giorgio, and E. Chioccarelli. 2013. Gamma degradation models for earthquake-resistant structures. *Structural Safety* 45: 48–58. doi:10.1016/j.strusafe.2013.09.001.
- Iervolino, I., and M. Dolce. 2018. Foreword to the special issue for the RINTC (the implicit seismic risk of code-conforming structures) project. *Journal of Earthquake Engineering* 22: 1–4. doi:10.1080/13632469.2018.1543697.
- Iervolino, I., A. Spillatura, and P. Bazzurro. 2018. Seismic reliability of code-conforming Italian buildings. *Journal of Earthquake Engineering* 22: 5–27. doi:10.1080/13632469.2018.1540372.
- Iervolino, I, R. Baraschino, A.Belleri, D. Cardone, G.Della Corte, P. Franchin, S.Lagomarsino, G.Magliulo, A.Marchi, A. Penna, L. R. S.Viggiani, and A. Zona. 2021. Seismic fragility of Italian code-conforming buildings by multi-stripe dynamic analysis of three-dimensional structural models. *Journal of Earthquake Engineering* (in review)
- Iervolino, I. 2022. Estimation uncertainty for some common seismic fragility curve fitting methods. *Soil Dynamics and Earthquake Engineering* 152: 107068. doi:10.1016/j.soildyn.2021.107068.
- Iovino M, Noto F, Di Laora R, de Sanctis L and Franchin P. (2022). Seismic Demand on Mid-Twentieth Century Reinforced Concrete Buildings Founded on Piles: Effect of Soil-Foundation-Structure-Interaction. *Journal of Earthquake Engineering*, 1–16. doi:10.1080/13632469.2022.2038728
- Jalayer, F., and C. A. Cornell. 2009. Alternative non-linear demand estimation methods for probability-based seismic assessments. *Earthquake Engineering & Structural Dynamics* 38: 951–72. doi:10.1002/eqe.876.
- Jalayer, F, I Iervolino, and G Manfredi. 2010. Structural modeling uncertainties and their influence on seismic assessment of existing RC structures. *Structural Safety* 32: 220–28. doi:10.1016/j.strusafe.2010.02.004.
- Jalayer F, et al 2011. Knowledge-Based Performance Assessment of Existing RC Buildings. *Journal of Earthquake Engineering*, 15(3): 362–389. doi:10.1080/13632469.2010.501193
- Lagomarsino, S., A. Penna, A. Galasco, and S. Cattari. 2013. TREMURI program: An equivalent frame model for the nonlinear seismic analysis of masonry buildings. *Engineering Structures* 56: 1787–99. doi:10.1016/j.engstruct.2013.08.002.
- Lagomarsino S, Cattari S, Angiolilli M, Bracchi S, Rota M and Penna A. (2022). Modelling and Seismic Response Analysis of Existing URM Structures. Part 2: Archetypes of Italian Historical Buildings. *Journal of Earthquake Engineering*, 1–26. doi:10.1080/13632469.2022.2087800
- Legge 25 novembre. 1962. Legge n°1684. Provvedimenti per l’edilizia con particolari prescrizioni per le zone sismiche. *Gazz Uff della REPUBB Ital GU* 326. (in Italian)
- Lin, T., C. B. Haselton, and J. W. Baker. 2013. Conditional spectrum-based ground motion selection. Part I: Hazard consistency for risk-based assessments. *Earthquake Engineering & Structural Dynamics* 42: 1847–65. doi:10.1002/eqe.2301.
- Luzi, L., S. Hailemikael, D. Bindi, F. Pacor, F. Mele, F. Sabetta. 2008. ITACA (Italian ACcelerometric Archive) : A web portal for the dissemination of Italian strong-motion data. *Seismological Research Letters* 79: 716–22. doi:10.1785/gssrl.79.5.716.
- McKenna, F., G. L. Fenves, M. H. Scott, and B. Jeremic. 2000. Open system for earthquake engineering simulation (OpenSees)
- Meletti, C., F. Galadini, G. Valensise, M. Stucchi, R. Basili, S. Barba, G. Vannucci, E. Boschi. 2008. A seismic source zone model for the seismic hazard assessment of the Italian territory. *Tectonophysics* 450 (1–4): 85–108. doi:10.1016/j.tecto.2008.01.003.
- Micozzi F, Flora A, Viggiani L, Cardone D, Ragni L and Dall’Asta A. 2021. Risk Assessment of Reinforced Concrete Buildings with Rubber Isolation Systems Designed by the Italian Seismic Code. *Journal of Earthquake Engineering*, 1–31. doi:10.1080/13632469.2021.1961937
- M.LL.PP. 1974. Legge n°64 del 2 febbraio 1974. Provvedimenti per le costruzioni con particolari prescrizioni per le zone sismiche. *Gazz Uff della REPUBB Ital GU* 64:1-9. (in Italian)
- M.LL.PP. 1997. Circolare n°65/AA .GG. del 10 Aprile 1997. Istruzioni per l’applicazione delle «Norme tecniche per le costruzioni in zone sismiche» di cui al decreto ministeriale 16 gennaio 1996. *Gazz Uff della REPUBB Ital GU* 97:1-30. (in Italian)
- Monelli, D., M. Pagani, G. Weatherill, Silva, V. and Crowley, H. 2012. The hazard component of openquake: The calculation engine of the global earthquake model. 15th World Conference Earthquake Engineering Lisbon, Portugal. doi:10.13140/2.1.3307.1364
- OPCM 3274. 2003. Primi elementi in materia di criteri generali per la classificazione sismica del territorio nazionale e di normative tecniche per le costruzioni in zona sismica. *Gazz Uff della REPUBB Ital GU* 105. (in Italian)

- OPCM 3431. 2005. Ordinanza del Presidente del Consiglio dei Ministri n. 3431 del 3/5/2005, Ulteriori modifiche ed integrazioni all'ordinanza del Presidente del Consiglio dei Ministri n. 3274 del 20 marzo 2003. Gazz Uff della Repubblica Ital GU. (in Italian)
- Penna, A., M. Rota, S. Bracchi, Angiolilli, M., Cattari, S., and Lagomarsino, S. 2022. Modelling and seismic response analysis of existing URM structures. Part 1: Modern buildings. *Journal of Earthquake Engineering* (in press)
- Petruzzelli, F., and I. Iervolino. 2021. NODE: A large-scale seismic risk prioritization tool for Italy based on nominal structural performance. *Bulletin of Earthquake Engineering* 19: 2763–96. doi:10.1007/s10518-021-01093-1.
- Pinto, A. V., G. Tsionis, E. Mola, and F. Taucer. 2003. Preliminary investigation of the Molise (Italy) earthquakes of 31 October and 1 November 2002. *Bulletin of Earthquake Engineering* 13 (1): 349–70. doi:10.1023/B:BEEE.0000021425.85961.F7.
- Ragni, L., D. Cardone, N. Conte, A. Dall'Asta, A. Di Cesare, A. Flora, G. Leccese, F. Micozzi, C. Ponso. 2018. Modeling and seismic response analysis of Italian code-conforming base-isolated buildings. *Journal of Earthquake Engineering* 22. doi:10.1080/13632469.2018.1527263
- Regio Decreto. 1909. R.D. 18 aprile 1909 n.193: Portante norme tecniche ed igieniche obbligatorie per le riparazioni ricostruzioni e nuove costruzioni degli edifici pubblici e privati nei luoghi colpiti dal terremoto del 28 dicembre 1908 e da altri precedenti elencati nel R.D. Gazz Uff del Regno d'Italia. (in Italian)
- Regio Decreto Legge. 1915. R.D.L. 29 aprile 1915 n.573: Norme tecniche ed igieniche da osservarsi per i lavori edilizi nelle località colpite dal terremoto del 13 gennaio 1915. Gazz Uff del Regno d'Italia 117. (in Italian)
- Regio Decreto Legge. 1935. R.D.L. 25 marzo 1935 n.573: Speciali prescrizioni per le località colpite dai terremoti. Gazz Uff del Regno d'Italia 120. (in Italian)
- Regio Decreto Legge. 1937. R.D.L. 22 novembre 1937 n.2105: Norme tecniche di edilizia con speciali prescrizioni per le località colpite dai terremoti. Gazz Uff del Regno d'Italia 298. (in Italian)
- Scozzese, F., G. Terracciano, A. Zona, G. D. Corte, A. Dall'Asta, R. Landolfo. 2018. Modeling and seismic response analysis of Italian code-conforming single-storey steel buildings. *Journal of Earthquake Engineering* 22: 2104–33. doi:10.1080/13632469.2018.1528913.
- Shome, N., and C. A. Cornell. 2000. Structural seismic demand analysis: Consideration of collapse. 8th ACSE Specialty Conference on Probabilistic Mechanics and Structural Reliability. South Bend, Indiana: University of Notre Dame. PMC2000–119
- Spillatura, A., M. Kohrangi, P. Bazzurro, and D. Vamvatsikos. 2021. Conditional spectrum record selection faithful to causative earthquake parameter distributions. *Earthquake Engineering & Structural Dynamics* 50: 2653–71. doi:10.1002/eqe.3465.
- Stucchi, M., C. Meletti, V. Montaldo, H. Crowley, G. M. Calvi, E. Boschi. 2011. Seismic hazard assessment (2003-2009) for the Italian building code. *Bulletin of the Seismological Society of America* 101: 1885–911. doi:10.1785/0120100130.
- Tomažević, M. 1978. *The computer program POR*. Ljubljana, Slovenia: Rep ZRMK (in Slovene).
- Vamvatsikos, D., and C. A. Cornell. 2002. Incremental dynamic analysis. *Earthquake Engineering & Structural Dynamics* 31: 491–514. doi:10.1002/eqe.141.
- Vamvatsikos, D., and C. A. Cornell. 2005. Developing efficient scalar and vector intensity measures for IDA capacity estimation by incorporating elastic spectral shape information. *Earthquake Engineering & Structural Dynamics* 34: 1573–600. doi:10.1002/eqe.496.
- Vamvatsikos, D. 2017. Performance-based seismic design in real life: The good, the bad and the ugly. XVII Convegno ANIDIS “L'Ingegneria Sismica in Italia” Pistoia, Italy.

Appendix

For portability of the vulnerability results herein presented, fragility curves are also fitted through the data from nonlinear dynamic analysis, as discussed in the next section. The fragility fitting framework is that referred to as *EDP*-based according to the terminology of Vamvatsikos and Cornell (2005), that is, starting from the results of MSA, the fragility is evaluated as the probability that the *EDP* random variable defined, conditional to fixed *IM* levels, is larger than the capacity. The *IM* to express the fragility is the same as the one to carry out MSA for the considered structural model, that is, spectral pseudo-acceleration at a vibration period close to the fundamental one.

Three fragility fitting procedures, described in details in Iervolino (2022), were considered: (i) *maximum likelihood* or ML; (ii) *Normal probability plot* or NPP; (iii) and (minimum) *least squares* or LSF, are considered. In fact, although ML is generally the preferred method, one of the other two had to be chosen in those cases when ML had convergence issues. The fitting results are given from Tables A1-A5, for all the buildings belonging to the investigated structural typologies (URM, RC, BI, PRC, and S), via the following information.

- *ID-building* containing fundamental information to identify the structure, such as typology, number of floors, site, and soil condition. It consists of two columns: the left one reporting the ID as expressed in Fig. 9, the right one providing details needed for the identification of each investigated structure.
- *Performance* identifies one between global collapse (GC) and usability-preventing damage (UPD).
- *Fitting* identifies the method used to evaluate the parameters of lognormal fragility.
- *IM* is the intensity measure respect of which fragility curves are evaluated.
- η identifies the mean of the logarithms of the *IM* causing structural failure.
- β identifies the standard deviation of the logarithms of the *IM* causing structural failure.
- λ_f identifies the failure rate.

Table A1. Fragilities and rates of failure for URM buildings. The ID-building is structured as follows: typology, design epoch, and code employed for performance upgrading, if any (left column); building identification number (BIN, if more than one building has been designed in the same design epoch per site) and/or failure mechanism (FM, if more than one exists), soil class and construction site (right column).

ID-building	Performance	Fitting	IM	η	β	λ_f	
URM_Pre-'20-NTC18	BIN1_C_NA	GC	ML	<i>Sa</i> (0.25s)	0.526	0.508	1.89E-04
		UPD	ML	<i>Sa</i> (0.25s)	-0.853	0.401	5.06E-03
URM_Pre-'20-POR	BIN1_C_NA	GC	ML	<i>Sa</i> (0.25s)	0.136	0.556	6.86E-04
		UPD	ML	<i>Sa</i> (0.25s)	-0.758	0.437	4.38E-03
URM_Pre-'20-CST ^a	BIN1_C_NA	GC	ML	<i>Sa</i> (0.25s)	-0.387	0.481	2.05E-03
		UPD	ML	<i>Sa</i> (0.25s)	-0.842	0.342	4.51E-03
URM_'20-'45-NTC18	BIN2_C_NA	GC	ML	<i>Sa</i> (0.25s)	-0.079	0.462	9.00E-04
		UPD	ML	<i>Sa</i> (0.25s)	-0.538	0.470	2.85E-03
URM_'20-'45-POR	BIN2_C_NA	GC	ML	<i>Sa</i> (0.25s)	-0.183	0.420	1.06E-03
		UPD	ML	<i>Sa</i> (0.25s)	-0.718	0.383	3.64E-03
URM_'45-'87	C_CT	GC	ML	<i>Sa</i> (0.50s)	0.391	0.426	4.33E-04
		UPD	ML	<i>Sa</i> (0.50s)	-1.691	0.058	1.32E-02
URM_Pre-'20	FM1_A_AQ	GC	ML	<i>Sa</i> (0.15s)	-0.336	0.600	3.69E-03
		UPD	ML	<i>Sa</i> (0.15s)	-0.781	0.382	6.06E-03
URM_Pre-'20	FM1_C_CT	GC	ML	<i>Sa</i> (0.50s)	0.139	0.478	7.18E-04
		UPD	ML	<i>Sa</i> (0.50s)	-1.357	0.444	9.72E-03
URM_'45-'87	C_MI	GC	ML	<i>Sa</i> (0.15s)	0.093	0.771	4.40E-05
		UPD	ML	<i>Sa</i> (0.15s)	-1.693	0.216	9.62E-04
URM_'20-'45	A_AQ	GC	ML	<i>Sa</i> (0.15s)	-0.204	0.293	1.23E-03
		UPD	ML	<i>Sa</i> (0.15s)	-1.309	0.415	2.06E-02
URM_'20-'45-CST	BIN1_AQ	GC	ML	<i>Sa</i> (0.15s)	-0.235	0.508	2.23E-03
		UPD	ML	<i>Sa</i> (0.15s)	-1.262	0.595	2.63E-02
URM_'20-'45-NTC18	BIN1_A_AQ	GC	ML	<i>Sa</i> (0.15s)	-0.098	0.442	1.32E-03
		UPD	ML	<i>Sa</i> (0.15s)	-0.948	0.503	1.13E-02
URM_'20-'45-POR	BIN1_A_AQ	GC	ML	<i>Sa</i> (0.15s)	-0.186	0.472	1.79E-03
		UPD	ML	<i>Sa</i> (0.15s)	-1.611	0.625	5.37E-02
URM_Post-'87	BIN1- FM1_C_RM	GC	ML	<i>Sa</i> (0.15s)	0.304	0.350	5.93E-05
		UPD	ML	<i>Sa</i> (0.15s)	-0.996	0.215	3.02E-03

(Continued)

Table A1. (Continued).

ID-building		Performance	Fitting	IM	η	β	λ_f
URM_Post-'87	BIN2- FM1_C_RM	GC	ML	<i>Sa</i> (0.15s)	-0.108	0.404	3.31E-04
		UPD	ML	<i>Sa</i> (0.15s)	-1.009	0.219	3.14E-03
URM_Pre-'20-NTC18	C_RM	GC	ML	<i>Sa</i> (0.50s)	-0.710	0.444	1.07E-03
		UPD	ML	<i>Sa</i> (0.50s)	-2.274	0.298	2.86E-02
URM_Pre-'20-CST	C_RM	GC	ML	<i>Sa</i> (0.50s)	-1.108	0.357	2.44E-03
		UPD	ML	<i>Sa</i> (0.50s)	-2.274	0.298	2.86E-02
URM_Pre-'20	FM2_C_CT	GC	ML	<i>Sa</i> (0.50s)	-0.186	0.512	1.34E-03
		UPD	ML	<i>Sa</i> (0.50s)	-1.357	0.444	9.72E-03
URM_Pre-'20	FM2_A_AQ	GC	ML	<i>Sa</i> (0.15s)	-0.245	0.450	1.95E-03
		UPD	ML	<i>Sa</i> (0.15s)	-0.971	0.416	9.95E-03
URM_Post-'87	BIN2-FM2_C_RM	GC	ML	<i>Sa</i> (0.15s)	0.210	0.497	1.76E-04
		UPD	ML	<i>Sa</i> (0.15s)	-0.581	0.271	1.00E-03
URM_'20-'45	C_MI	GC	LSF	<i>Sa</i> (0.15s)	-0.336	0.273	6.97E-06
		UPD	ML	<i>Sa</i> (0.15s)	-1.726	0.470	5.27E-03
URM_'20-'45-CST	BIN2_A_AQ	GC	ML	<i>Sa</i> (0.15s)	-0.211	0.496	2.03E-03
		UPD	ML	<i>Sa</i> (0.15s)	-1.504	0.264	2.53E-02
URM_'20-'45-NTC18	BIN2_A_AQ	GC	ML	<i>Sa</i> (0.15s)	0.122	0.584	1.17E-03
		UPD	ML	<i>Sa</i> (0.15s)	-0.878	0.283	6.44E-03
URM_'20-'45-POR	BIN2_A_AQ	GC	ML	<i>Sa</i> (0.15s)	-0.240	0.326	1.44E-03
		UPD	ML	<i>Sa</i> (0.15s)	-1.514	0.048	2.25E-02
URM_Post-'87	BIN1-FM2_C_RM	GC	ML	<i>Sa</i> (0.15s)	0.473	0.428	4.68E-05
		UPD	ML	<i>Sa</i> (0.15s)	-0.228	0.179	2.47E-04

Table A2. Fragilities and rates of failure for RC buildings. The ID-building is structured as follows: typology, number of stories and design epoch (left column); infilling type, soil class and construction site (right column).

ID-building		Performance	Fitting	IM	η	β	λ_f
RC_3_Pre-'70	BF_C_AQ	GC	ML	<i>Sa</i> (1.00s)	-1.017	0.328	2.20E-03
		UPD	ML	<i>Sa</i> (1.00s)	-1.987	0.054	8.99E-03
RC_3_Pre-'70	IF_C_AQ	GC	ML	<i>Sa</i> (1.00s)	-0.788	0.326	1.50E-03
		UPD	ML	<i>Sa</i> (1.00s)	-1.806	0.441	8.56E-03
RC_3_Pre-'70	PF_C_AQ	GC	ML	<i>Sa</i> (1.00s)	-0.825	0.543	2.03E-03
		UPD	ML	<i>Sa</i> (1.00s)	-1.635	0.204	5.42E-03
RC_6_Pre-'70	BF_C_AQ	GC	ML	<i>Sa</i> (1.00s)	-0.513	0.242	8.73E-04
		UPD	ML	<i>Sa</i> (1.00s)	-1.849	0.234	7.68E-03
RC_6_Pre-'70	IF_C_AQ	GC	ML	<i>Sa</i> (1.00s)	-0.633	0.372	1.20E-03
		UPD	ML	<i>Sa</i> (1.00s)	-1.667	0.235	5.79E-03
RC_6_Pre-'70	PF_C_AQ	GC	ML	<i>Sa</i> (1.00s)	-0.848	0.376	1.74E-03
		UPD	ML	<i>Sa</i> (1.00s)	-1.676	0.315	6.19E-03
RC_3_'70s	BF_C_AQ	GC	ML	<i>Sa</i> (1.00s)	-0.303	0.244	5.92E-04
		UPD	ML	<i>Sa</i> (1.00s)	-1.952	0.275	9.27E-03
RC_3_'70s	IF_C_AQ	GC	ML	<i>Sa</i> (1.00s)	-0.502	0.357	9.44E-04
		UPD	ML	<i>Sa</i> (1.00s)	-1.502	0.360	4.89E-03
RC_3_'70s	PF_C_AQ	GC	ML	<i>Sa</i> (1.00s)	-0.543	0.324	9.84E-04
		UPD	ML	<i>Sa</i> (1.00s)	-1.474	0.291	4.44E-03
RC_6_'70s	BF_C_AQ	GC	ML	<i>Sa</i> (1.00s)	-0.899	0.265	1.73E-03
		UPD	ML	<i>Sa</i> (1.00s)	-1.774	0.407	7.84E-03
RC_6_'70s	IF_C_AQ	GC	ML	<i>Sa</i> (1.00s)	-0.329	0.411	7.34E-04
		UPD	ML	<i>Sa</i> (1.00s)	-1.542	0.495	6.01E-03
RC_6_'70s	PF_C_AQ	GC	ML	<i>Sa</i> (1.00s)	-0.627	0.337	1.15E-03
		UPD	ML	<i>Sa</i> (1.00s)	-1.461	0.046	3.94E-03
RC_3_'80-'90	BF_C_AQ	GC	ML	<i>Sa</i> (1.00s)	0.177	0.313	2.41E-04
		UPD	ML	<i>Sa</i> (1.00s)	-1.752	0.341	7.12E-03
RC_3_'80-'90	IF_C_AQ	GC	ML	<i>Sa</i> (1.00s)	0.139	0.348	2.73E-04
		UPD	ML	<i>Sa</i> (1.00s)	-1.303	0.557	4.47E-03
RC_3_'80-'90	PF_C_AQ	GC	ML	<i>Sa</i> (1.00s)	0.027	0.299	3.25E-04
		UPD	ML	<i>Sa</i> (1.00s)	-1.258	0.427	3.55E-03
RC_6_'80-'90	BF_C_AQ	GC	ML	<i>Sa</i> (1.00s)	-0.347	0.327	6.92E-04
		UPD	ML	<i>Sa</i> (1.00s)	-1.703	0.337	6.57E-03

(Continued)

Table A2. (Continued).

ID-building		Performance	Fitting	IM	η	β	λ_f
RC_6_'80-'90	IF_C_AQ	GC	ML	Sa(1.00s)	0.212	0.316	2.24E-04
		UPD	ML	Sa(1.00s)	-1.258	0.233	3.04E-03
RC_6_'80-'90	PF_C_AQ	GC	ML	Sa(1.00s)	-0.457	0.397	9.09E-04
		UPD	ML	Sa(1.00s)	-1.211	0.194	2.77E-03
RC_3_Pre-'70	BF_C_CT	GC	ML	Sa(1.00s)	-0.639	0.432	7.58E-04
		UPD	ML	Sa(1.00s)	-2.081	0.265	6.68E-03
RC_3_Pre-'70	IF_C_CT	GC	ML	Sa(1.00s)	-0.626	0.474	7.79E-04
		UPD	ML	Sa(1.00s)	-2.122	0.413	8.12E-03
RC_3_Pre-'70	PF_C_CT	GC	ML	Sa(1.00s)	-0.756	0.476	9.66E-04
		UPD	ML	Sa(1.00s)	-1.659	0.420	3.89E-03
RC_6_Pre-'70	BF_C_CT	GC	ML	Sa(1.00s)	-0.710	0.400	8.22E-04
		UPD	ML	Sa(1.00s)	-1.987	0.220	5.57E-03
RC_6_Pre-'70	IF_C_CT	GC	ML	Sa(1.00s)	-0.326	0.471	4.73E-04
		UPD	ML	Sa(1.00s)	-1.682	0.636	5.39E-03
RC_6_Pre-'70	PF_C_CT	GC	ML	Sa(1.00s)	-0.343	0.741	7.47E-04
		UPD	ML	Sa(1.00s)	-1.476	0.788	5.10E-03
RC_3_'70s	BF_C_CT	GC	ML	Sa(1.00s)	-0.801	0.507	1.08E-03
		UPD	ML	Sa(1.00s)	-2.138	0.310	7.58E-03
RC_3_'70s	IF_C_CT	GC	ML	Sa(1.00s)	-0.555	0.412	6.46E-04
		UPD	ML	Sa(1.00s)	-2.076	0.495	8.29E-03
RC_3_'70s	PF_C_CT	GC	ML	Sa(1.00s)	-0.870	0.533	1.25E-03
		UPD	ML	Sa(1.00s)	-1.356	0.540	2.77E-03
RC_6_'70s	BF_C_CT	GC	ML	Sa(1.00s)	-0.162	0.378	3.22E-04
		UPD	ML	Sa(1.00s)	-1.723	0.313	3.89E-03
RC_6_'70s	IF_C_CT	GC	ML	Sa(1.00s)	-0.311	0.404	4.27E-04
		UPD	ML	Sa(1.00s)	-1.770	0.251	4.01E-03
RC_6_'70s	PF_C_CT	GC	ML	Sa(1.00s)	-0.250	0.355	3.66E-04
		UPD	ML	Sa(1.00s)	-1.741	0.184	3.68E-03
RC_3_'80-'90	BF_C_CT	GC	ML	Sa(1.00s)	0.358	0.518	1.53E-04
		UPD	ML	Sa(1.00s)	-1.869	0.842	1.05E-02
RC_3_'80-'90	IF_C_CT	GC	ML	Sa(1.00s)	0.303	0.490	1.62E-04
		UPD	ML	Sa(1.00s)	-1.373	0.687	3.59E-03
RC_3_'80-'90	PF_C_CT	GC	ML	Sa(1.00s)	0.256	0.508	1.81E-04
		UPD	ML	Sa(1.00s)	-1.189	0.654	2.52E-03
RC_6_'80-'90	BF_C_CT	GC	ML	Sa(1.00s)	-0.061	0.879	6.31E-04
		UPD	ML	Sa(1.00s)	-1.803	0.795	8.67E-03
RC_6_'80-'90	IF_C_CT	GC	ML	Sa(1.00s)	0.262	0.847	3.42E-04
		UPD	ML	Sa(1.00s)	-1.115	0.664	2.27E-03
RC_6_'80-'90	PF_C_CT	GC	ML	Sa(1.00s)	-0.169	0.817	6.55E-04
		UPD	ML	Sa(1.00s)	-1.062	0.725	2.33E-03
RC_3_Pre-'70	BF_C_MI	GC	LSF	Sa(1.00s)	1.024	1.083	3.14E-06
		UPD	ML	Sa(1.00s)	-1.788	0.506	2.91E-04
RC_3_Pre-'70	IF_C_MI	GC	ML	Sa(1.00s)	-1.203	0.063	7.57E-06
		UPD	ML	Sa(1.00s)	-1.460	0.569	1.43E-04
RC_3_Pre-'70	PF_C_MI	GC	LSF	Sa(1.00s)	-0.803	0.311	3.04E-06
		UPD	ML	Sa(1.00s)	-1.388	0.295	3.06E-05
RC_6_Pre-'70	BF_C_MI	GC	ML	Sa(1.00s)	-1.245	0.058	9.07E-06
		UPD	ML	Sa(1.00s)	-1.755	0.766	9.54E-04
RC_6_Pre-'70	IF_C_MI	GC	LSF	Sa(1.00s)	0.506	0.439	1.51E-08
		UPD	ML	Sa(1.00s)	-1.49	0.260	4.09E-05
RC_6_Pre-'70	PF_C_MI	GC	LSF	Sa(1.00s)	0.599	0.471	1.36E-08
		UPD	ML	Sa(1.00s)	-1.17	0.42	2.39E-05
RC_3_'70s	BF_C_MI	GC	LSF	Sa(1.00s)	-0.684	0.412	3.41E-06
		UPD	ML	Sa(1.00s)	-2.034	0.292	2.89E-04
RC_3_'70s	IF_C_MI	GC	ML	Sa(1.00s)	-1.203	0.063	7.57E-06
		UPD	ML	Sa(1.00s)	-1.310	0.746	2.46E-04
RC_3_'70s	PF_C_MI	GC	LSF	Sa(1.00s)	-0.351	0.528	2.08E-06
		UPD	ML	Sa(1.00s)	-1.284	0.402	3.38E-05
RC_6_'70s	BF_C_MI	GC	LSF	Sa(1.00s)	0.324	0.338	1.32E-08
		UPD	ML	Sa(1.00s)	-1.258	0.574	7.70E-05

(Continued)

Table A2. (Continued).

ID-building		Performance	Fitting	IM	η	β	λ_f
RC_6_'70s	IF_C_MI	GC	LSF	Sa(1.00s)	0.812	0.596	6.15E-09
		UPD	ML	Sa(1.00s)	-1.62	0.340	8.41E-05
RC_6_'70s	PF_C_MI	GC	ML	Sa(1.00s)	0.860	0.396	1.16E-09
		UPD	ML	Sa(1.00s)	-1.61	0.260	6.11E-05
RC_3_'80-'90	BF_C_MI	GC	LSF	Sa(1.00s)	0.312	0.458	5.20E-08
		UPD	ML	Sa(1.00s)	-1.572	0.340	7.17E-05
RC_3_'80-'90	IF_C_MI	GC	LSF	Sa(1.00s)	0.249	0.474	8.40E-08
		UPD	ML	Sa(1.00s)	-0.548	0.886	6.72E-05
RC_3_'80-'90	PF_C_MI	GC	LSF	Sa(1.00s)	0.003	0.501	3.57E-07
		UPD	ML	Sa(1.00s)	-1.245	0.058	9.07E-06
RC_6_'80-'90	BF_C_MI	GC	LSF	Sa(1.00s)	0.732	0.339	1.20E-09
		UPD	ML	Sa(1.00s)	-1.093	0.458	2.26E-05
RC_6_'80-'90	IF_C_MI	GC	LSF	Sa(1.00s)	1.363	0.466	1.61E-10
		UPD	ML	Sa(1.00s)	-1.35	0.310	2.92E-05
RC_6_'80-'90	PF_C_MI	GC	LSF	Sa(1.00s)	0.808	0.354	9.14E-10
		UPD	ML	Sa(1.00s)	-1.11	0.39	1.62E-05
RC_3_Pre-'70	BF_C_NA	GC	ML	Sa(1.00s)	-0.711	0.231	2.00E-04
		UPD	ML	Sa(1.00s)	-1.820	0.461	4.88E-03
RC_3_Pre-'70	IF_C_NA	GC	ML	Sa(1.00s)	-0.652	0.289	1.90E-04
		UPD	ML	Sa(1.00s)	-1.770	0.564	5.18E-03
RC_3_Pre-'70	PF_C_NA	GC	ML	Sa(1.00s)	-0.807	0.298	3.14E-04
		UPD	ML	Sa(1.00s)	-1.422	0.361	1.81E-03
RC_6_Pre-'70	BF_C_NA	GC	ML	Sa(1.00s)	-0.600	0.490	3.03E-04
		UPD	ML	Sa(1.00s)	-2.063	0.507	8.04E-03
RC_6_Pre-'70	IF_C_NA	GC	ML	Sa(1.00s)	-0.347	0.251	6.12E-05
		UPD	ML	Sa(1.00s)	-1.537	0.314	2.20E-03
RC_6_Pre-'70	PF_C_NA	GC	ML	Sa(1.00s)	-0.399	0.294	8.35E-05
		UPD	ML	Sa(1.00s)	-0.911	0.596	9.33E-04
RC_3_'70s	BF_C_NA	GC	ML	Sa(1.00s)	-0.888	0.270	3.75E-04
		UPD	ML	Sa(1.00s)	-1.977	0.508	6.94E-03
RC_3_'70s	IF_C_NA	GC	ML	Sa(1.00s)	-0.657	0.227	1.66E-04
		UPD	ML	Sa(1.00s)	-1.739	0.650	5.64E-03
RC_3_'70s	PF_C_NA	GC	ML	Sa(1.00s)	-0.877	0.325	4.11E-04
		UPD	ML	Sa(1.00s)	-1.241	0.380	1.22E-03
RC_6_'70s	BF_C_NA	GC	ML	Sa(1.00s)	-0.134	0.316	3.52E-05
		UPD	ML	Sa(1.00s)	-1.733	0.404	3.81E-03
RC_6_'70s	IF_C_NA	GC	ML	Sa(1.00s)	-0.333	0.207	5.13E-05
		UPD	ML	Sa(1.00s)	-1.720	0.330	3.36E-03
RC_6_'70s	PF_C_NA	GC	ML	Sa(1.00s)	-0.146	0.253	2.92E-05
		UPD	ML	Sa(1.00s)	-1.566	0.225	2.12E-03
RC_3_'80-'90	BF_C_NA	GC	ML	Sa(1.00s)	-0.238	0.298	4.80E-05
		UPD	ML	Sa(1.00s)	-1.700	0.442	3.76E-03
RC_3_'80-'90	IF_C_NA	GC	ML	Sa(1.00s)	-0.089	0.207	2.01E-05
		UPD	ML	Sa(1.00s)	-1.105	0.584	1.40E-03
RC_3_'80-'90	PF_C_NA	GC	ML	Sa(1.00s)	-0.170	0.206	2.76E-05
		UPD	ML	Sa(1.00s)	-0.928	0.382	5.45E-04
RC_6_'80-'90	BF_C_NA	GC	ML	Sa(1.00s)	0.023	0.230	1.38E-05
		UPD	ML	Sa(1.00s)	-1.564	0.446	2.86E-03
RC_6_'80-'90	IF_C_NA	GC	ML	Sa(1.00s)	-0.013	0.319	2.26E-05
		UPD	ML	Sa(1.00s)	-1.318	0.348	1.39E-03
RC_6_'80-'90	PF_C_NA	GC	ML	Sa(1.00s)	0.036	0.045	8.61E-06
		UPD	ML	Sa(1.00s)	-1.345	0.268	1.31E-03

Table A3. Fragilities and rates of failure for BI buildings. The ID-building is structured as follows: typology, isolation system typology, and design epoch (left column); soil class and construction site (right column).

ID-building		Performance	Fitting	IM	η	β	λ_f
BI_FPS_Pre-70	C_AQ	GC	ML	Sa(3.00s)	-1.520	0.200	4.35E-04
		UPD	ML	Sa(3.00s)	-1.882	0.522	1.18E-03
BI_FPS_70s	C_AQ	GC	ML	Sa(3.00s)	-1.500	0.215	4.22E-04
		UPD	ML	Sa(3.00s)	-1.641	0.283	5.97E-04
BI_FPS_80-90	C_AQ	GC	ML	Sa(3.00s)	-1.389	0.259	3.46E-04
		UPD	ML	Sa(3.00s)	-1.389	0.259	3.46E-04
BI_HDRD+S_Pre-70	C_AQ	GC	ML	Sa(3.00s)	-1.477	0.194	3.95E-04
		UPD	ML	Sa(3.00s)	-1.859	0.451	1.05E-03
BI_HDRD+S_70s	C_AQ	GC	ML	Sa(3.00s)	-1.335	0.044	2.67E-04
		UPD	ML	Sa(3.00s)	-1.632	0.315	6.94E-04
BI_HDRD+S_80-90	C_AQ	GC	ML	Sa(3.00s)	-1.290	0.221	2.67E-04
		UPD	ML	Sa(3.00s)	-1.661	0.288	6.24E-04
BI_FPS_Pre-70	C_NA	GC	ML	Sa(3.00s)	-1.660	0.271	8.80E-05
		UPD	ML	Sa(3.00s)	-2.283	0.279	5.25E-04
BI_FPS_70s	C_NA	GC	ML	Sa(3.00s)	-1.594	0.194	5.97E-05
		UPD	ML	Sa(3.00s)	-1.979	0.347	2.68E-04
BI_FPS_80-90	C_NA	GC	ML	Sa(3.00s)	-1.519	0.036	3.74E-05
		UPD	ML	Sa(3.00s)	-1.764	0.399	1.69E-04
BI_HDRD+S_Pre-70	C_NA	GC	ML	Sa(3.00s)	-1.715	0.303	1.13E-04
		UPD	ML	Sa(3.00s)	-2.140	0.310	3.82E-04
BI_HDRD+S_70s	C_NA	GC	ML	Sa(3.00s)	-1.598	0.278	7.33E-05
		UPD	ML	Sa(3.00s)	-2.071	0.325	3.68E-04
BI_HDRD+S_80-90	C_NA	GC	ML	Sa(3.00s)	-1.507	0.240	4.90E-05
		UPD	ML	Sa(3.00s)	-1.870	0.249	1.61E-04

Table A4. Fragilities and rates of failure for PRC buildings. The ID-building is structured as follows: typology, structural system, and design epoch (left column); soil class and construction site (right column).

ID-building		Performance	Fitting	IM	η	β	λ_f
PRC_EE2_80-90	C_AQ	GC	ML	Sa(2.00s)	-2.056	0.447	2.36E-03
		UPD	ML	Sa(2.00s)	-2.256	0.331	2.92E-03
PRC_EE2_80-90	C_MI	GC	LSF	Sa(2.00s)	2.080	0.235	1.86E-18
		UPD	ML	Sa(2.00s)	-3.375	0.326	1.28E-03
PRC_EE2_80-90	C_NA	GC	ML	Sa(2.00s)	-1.163	0.281	3.54E-05
		UPD	ML	Sa(2.00s)	-2.588	0.372	3.03E-03
PRC_EE1_70s	C_NA	GC	ML	Sa(0.50s)	1.388	0.708	2.06E-05
		UPD	ML	Sa(0.50s)	-0.881	0.497	3.46E-03
PRC_EE1_70s	C_MI	GC	LSF	Sa(0.50s)	0.233	0.275	5.97E-07
		UPD	ML	Sa(0.50s)	-0.696	0.492	9.93E-05
PRC_EE1_Pre-70	C_AQ	GC	LSF	Sa(0.50s)	0.084	0.636	1.90E-03
		UPD	ML	Sa(0.50s)	-0.435	0.324	2.97E-03
PRC_EE1_70s	C_AQ	GC	ML	Sa(0.50s)	0.023	0.563	1.80E-03
		UPD	ML	Sa(0.50s)	-0.456	0.407	3.39E-03
PRC_EE3_70s	C_AQ	GC	ML	Sa(0.50s)	0.623	0.566	6.09E-04
		UPD	ML	Sa(0.50s)	-0.894	0.335	6.75E-03
PRC_EE3_70s	C_MI	GC	LSF	Sa(0.50s)	0.069	0.167	7.69E-07
		UPD	ML	Sa(0.50s)	-0.652	0.048	1.66E-05
PRC_EE3_70s	C_NA	GC	ML	Sa(0.50s)	1.705	0.934	3.52E-05
		UPD	ML	Sa(0.50s)	-0.702	0.286	1.62E-03
PRC_EE4_80-90	C_AQ	GC	ML	Sa(3.00s)	-2.395	0.331	2.25E-03
		UPD	ML	Sa(3.00s)	-3.364	0.484	8.59E-03
PRC_EE4_80-90	C_MI	GC	ML	Sa(3.00s)	-2.412	0.077	7.22E-07
		UPD	ML	Sa(3.00s)	-3.118	0.041	6.21E-06
PRC_EE4_80-90	C_NA	GC	ML	Sa(3.00s)	-2.429	0.444	9.50E-04
		UPD	ML	Sa(3.00s)	-3.298	0.302	4.00E-03

Table A5. Fragilities and rates of failure for steel buildings. The ID-building is structured as follows: typology, structural scheme in transversal direction and envelope panels type (left column); structural scheme in longitudinal direction, soil class and construction site (right column).

ID-building		Performance	Fitting	IM	η	β	λ_f
S_PCB-BF	L_C_AQ	GC	ML	<i>Sa</i> (1.00s)	0.614	0.047	6.85E-05
		UPD	ML	<i>Sa</i> (1.00s)	-	-	-
S_PCB-SP	L_C_AQ	GC	ML	<i>Sa</i> (0.50s)	0.972	0.329	2.06E-04
		UPD	ML	<i>Sa</i> (0.50s)	0.729	0.261	3.17E-04
S_PCB-TS	L_C_AQ	GC	ML	<i>Sa</i> (0.50s)	0.712	0.349	3.62E-04
		UPD	ML	<i>Sa</i> (0.50s)	-1.330	0.227	1.33E-02
S_PCB-BF ⁹	SHS_C_AQ	GC	ML	<i>Sa</i> (1.00s)	0.708	0.284	6.75E-05
		UPD	ML	<i>Sa</i> (1.00s)	-	-	-
S_PCB-BF	SHS_C_MI	GC	LSF	<i>Sa</i> (1.00s)	24.694	7.338	5.73E-06
		UPD	ML	<i>Sa</i> (1.00s)	-	-	-
S_PCB-BF	SHS_C_NA	GC	ML	<i>Sa</i> (1.00s)	0.079	0.049	7.16E-06
		UPD	ML	<i>Sa</i> (1.00s)	-	-	-
S_PCB-SP	SHS_C_AQ	GC	ML	<i>Sa</i> (0.50s)	1.022	0.430	2.16E-04
		UPD	ML	<i>Sa</i> (0.50s)	0.711	0.248	3.25E-04
S_PCB-SP	SHS_C_MI	GC	LSF	<i>Sa</i> (0.50s)	23.670	6.843	1.56E-05
		UPD	LSF	<i>Sa</i> (0.50s)	-0.226	0.116	2.75E-06
S_PCB-SP	SHS_C_NA	GC	ML	<i>Sa</i> (0.50s)	2.607	1.140	1.31E-05
		UPD	ML	<i>Sa</i> (0.50s)	0.606	0.396	4.84E-05
S_PCB-TS	SHS_C_AQ	GC	ML	<i>Sa</i> (0.50s)	0.756	0.395	3.53E-04
		UPD	ML	<i>Sa</i> (0.50s)	-1.357	0.213	1.38E-02
S_PCB-TS	SHS_C_MI	GC	LSF	<i>Sa</i> (0.50s)	-0.219	0.110	2.62E-06
		UPD	ML	<i>Sa</i> (0.50s)	-0.729	0.275	3.99E-05
S_PCB-TS	SHS_C_NA	GC	ML	<i>Sa</i> (0.50s)	0.630	0.448	4.85E-05
		UPD	ML	<i>Sa</i> (0.50s)	-0.927	0.330	2.92E-03
S_SCB-BF	L_C_AQ	GC	ML	<i>Sa</i> (1.00s)	0.585	0.474	1.29E-04
		UPD	ML	<i>Sa</i> (1.00s)	-	-	-
S_SCB-SP	L_C_AQ	GC	ML	<i>Sa</i> (0.50s)	1.694	0.472	5.17E-05
		UPD	ML	<i>Sa</i> (0.50s)	0.848	0.282	2.53E-04
S_SCB-SP	L_C_MI	GC	LSF	<i>Sa</i> (0.50s)	23.670	6.843	1.56E-05
		UPD	ML	<i>Sa</i> (0.50s)	-0.072	0.170	1.55E-06
S_SCB-SP	L_C_NA	GC	LSF	<i>Sa</i> (0.50s)	1.441	0.196	8.14E-07
		UPD	LSF	<i>Sa</i> (0.50s)	1.029	0.246	5.59E-06
S_SCB-TS	L_C_AQ	GC	ML	<i>Sa</i> (0.50s)	1.146	0.400	1.57E-04
		UPD	ML	<i>Sa</i> (0.50s)	-0.604	0.262	3.79E-03
S_SCB-BF	SHS_C_AQ	GC	ML	<i>Sa</i> (1.00s)	1.093	0.589	5.33E-05
		UPD	ML	<i>Sa</i> (1.00s)	-	-	-
S_SCB-SP	SHS_C_AQ	GC	ML	<i>Sa</i> (0.50s)	1.720	0.460	4.71E-05
		UPD	ML	<i>Sa</i> (0.50s)	1.071	0.418	1.91E-04
S_SCB-TS	SHS_C_AQ	GC	ML	<i>Sa</i> (0.50s)	1.571	0.578	9.02E-05
		UPD	ML	<i>Sa</i> (0.50s)	-0.623	0.269	3.94E-03